Maximum Intensity Projection (MIP) of a chip of Nakhla obtained at the Institute of Anatomy (University of Bern, Switzerland) using nano-XCT (4 microns per voxel size).

Searching for Micron- to Sub-Micron-Sized Glassy and C-rich Phases in Martian and Carbonaceous Meteorites

Dr. Pierre-Etienne M. C. MARTIN

Astronomical Institute of the Romanian Academy Scientific Seminar

28th of January 2026

UNIVERSITÄT BERN

PlanetS National Centre of Competence in Research

Schweizerischer Nationalfonds

Copyright Disclaimer

Discretion is advised in this presentation due to some sections remaining currently unpublished (16/02/2026).

This a formal notification that the material being presented contains preliminary, sensitive, or proprietary data.

The ideas or data should not be copied, shared, or cited without the author's permission.

Thank you.

– Pierre-Etienne Martin, 2026

Background

- **Post-doctoral Research Assistant**
  Natural History Museum, London (UK)

- **Ph.D. in Planetary Sciences**
  University of Glasgow (UK)

- **MSc *cum laude* in Earth and Planetary Sciences**
  Ecole Normale Supérieure de Lyon
  Université Paris VII
  Institut de Physique du Globe de Paris

- **BSc in Geology**
  Université du Québec à Chicoutimi (Canada)

Research Interests

- Cosmochemistry and astrobiology
- Origin of water and volatile elements
- Meteorites and asteroids
- CAIs (Calcium-Aluminium-rich Inclusions)

Background

- **Post-doctoral Research Assistant**
  Natural History Museum, London (UK)

- **Ph.D. in Planetary Sciences**
  University of Glasgow (UK)

- **MSc *cum laude* in Earth and Planetary Sciences**
  Ecole Normale Supérieure de Lyon
  Université Paris VII
  Institut de Physique du Globe de Paris

- **BSc in Geology**
  Université du Québec à Chicoutimi (Canada)

Mineralogical, textural, and geochemical characterisation of recent meteorite falls and samples returned from the carbonaceous asteroids Ryugu and Bennu

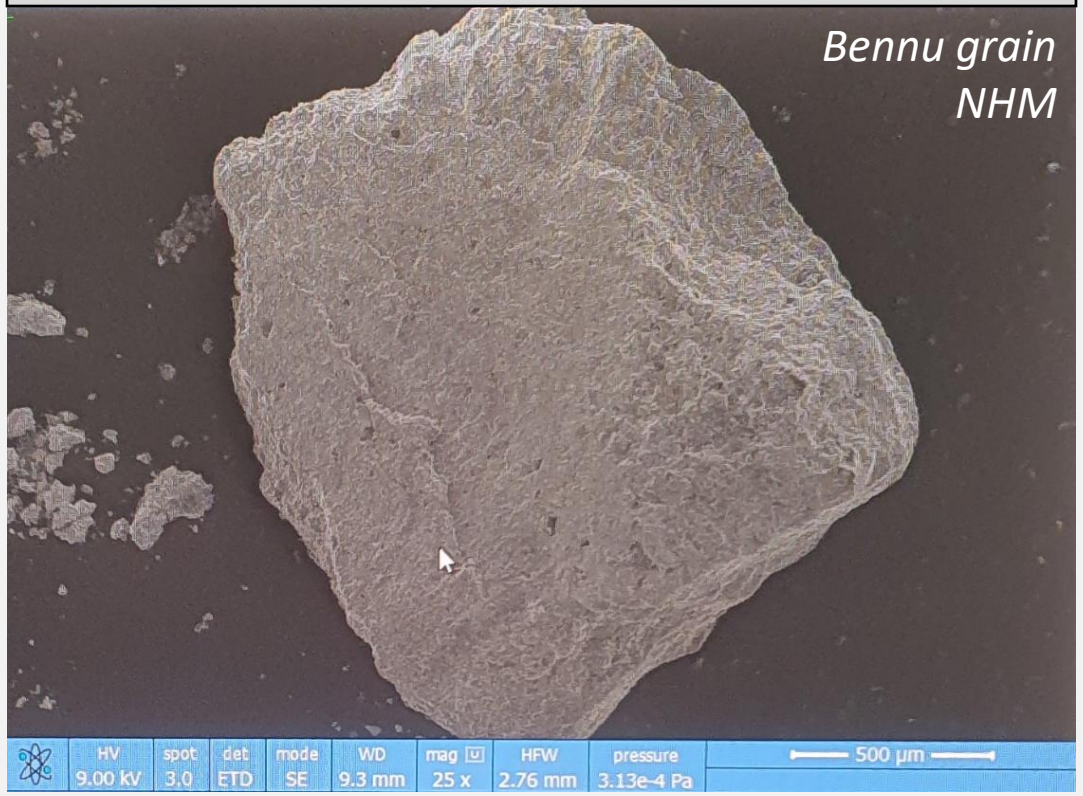

Research Interests

- Cosmochemistry and astrobiology
- Origin of water and volatile elements
- Meteorites and asteroids
- CAIs (Calcium-Aluminium-rich Inclusions)

Background

- **Post-doctoral Research Assistant**
  Natural History Museum, London (UK)

- **Ph.D. in Planetary Sciences**
  University of Glasgow (UK)

- **MSc *cum laude* in Earth and Planetary Sciences**
  Ecole Normale Supérieure de Lyon
  Université Paris VII
  Institut de Physique du Globe de Paris

- **BSc in Geology**
  Université du Québec à Chicoutimi (Canada)

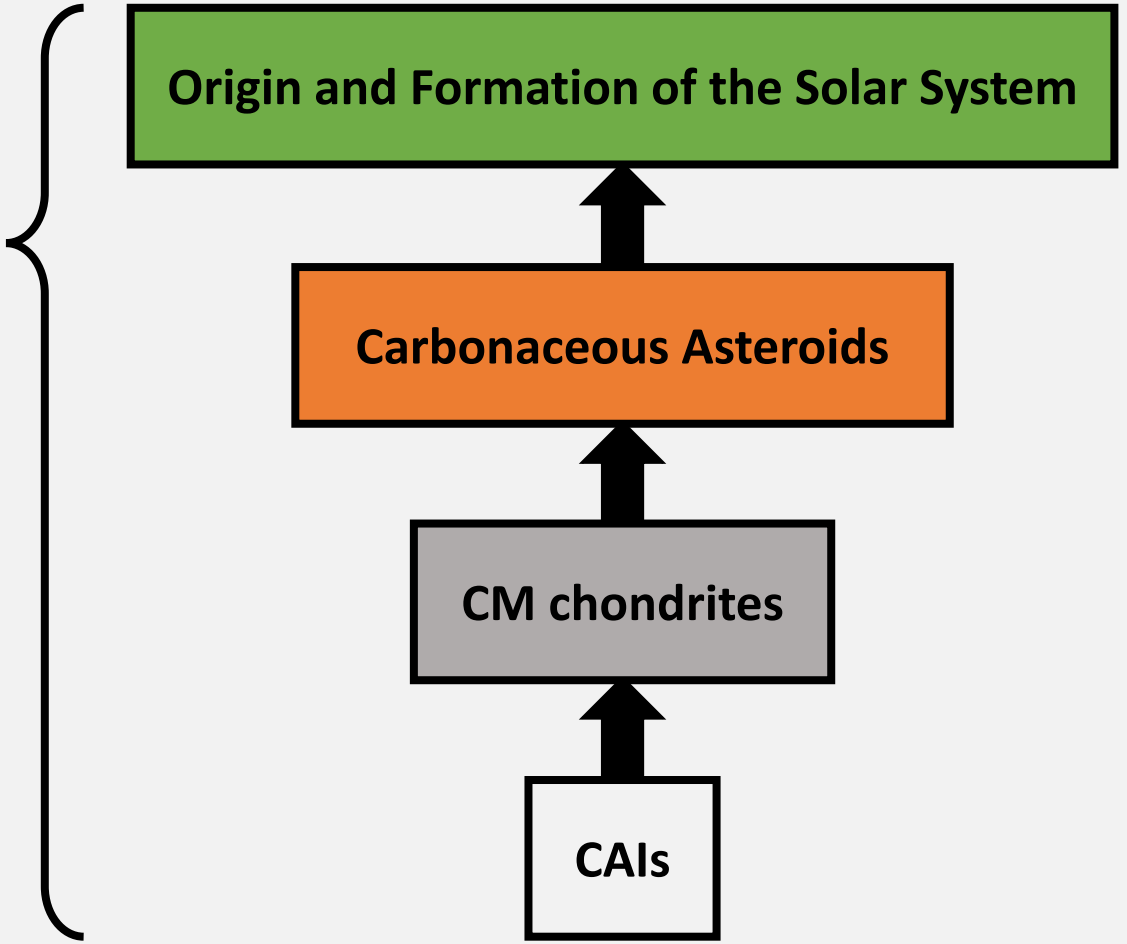

Research Interests

- Cosmochemistry and astrobiology
- Origin of water and volatile elements
- Meteorites and asteroids
- CAIs (Calcium-Aluminium-rich Inclusions)

C-type (Carbonaceous) Asteroids

- Asteroids are small bodies (m-km in size) made of rock and/or metal orbiting the Sun and are the surviving remnants (the "leftover crumbs") of **early planet formation processes** (Bottke et al. 2021; Carry 2012; Gaffey 2011).

- **Sample collection missions** (e.g. JAXA's Hayabusa2 and NASA's OSIRIS-Rex) aim to provide answers to questions regarding the **delivery of volatiles and organics to Earth**.

- **Carbonaceous chondrites** can be used as analogues to these asteroids (Wada et al., 2018; Schrader & Davidson, 2017).

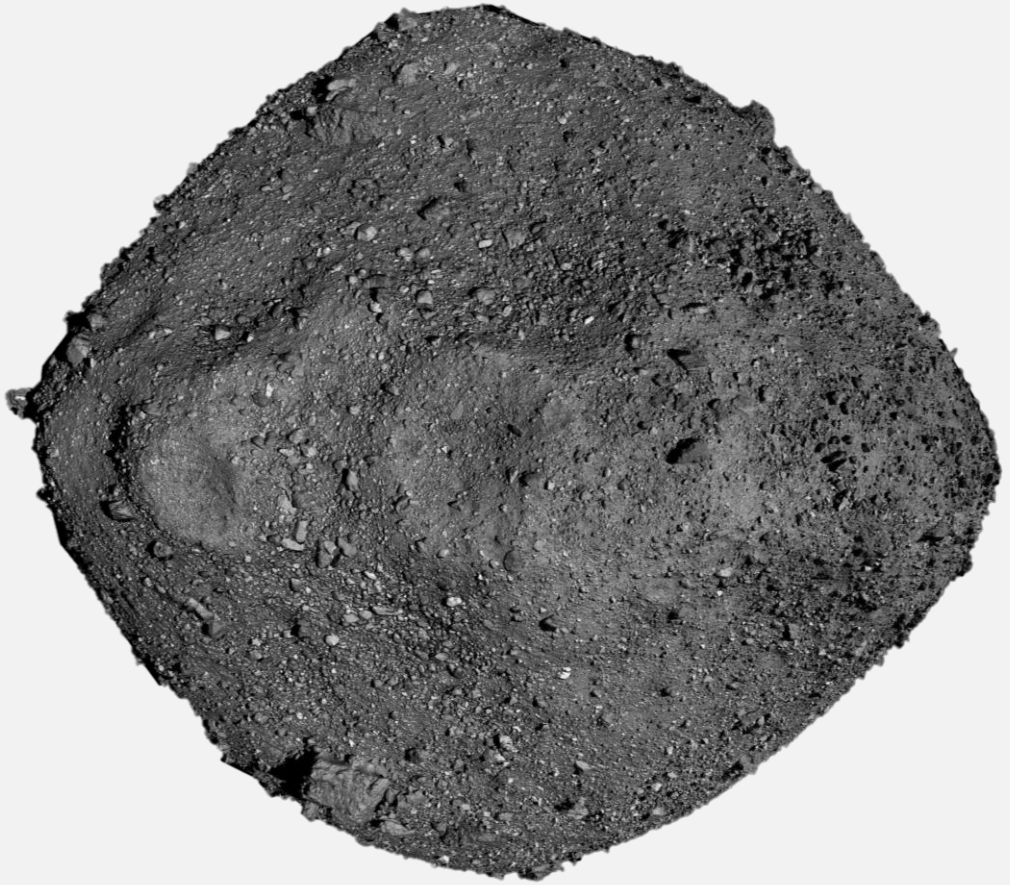

Credits: Asteroid Ryugu, JAXA

C-type (Carbonaceous) Asteroids

- Asteroids are small bodies (m-km in size) made of rock and/or metal orbiting the Sun and are the surviving remnants (the "leftover crumbs") of **early planet formation processes** (Bottke et al. 2021; Carry 2012; Gaffey 2011).

- **Sample collection missions** (e.g. JAXA's Hayabusa2 and NASA's OSIRIS-Rex) aim to provide answers to questions regarding the **delivery of volatiles and organics to Earth**.

- **Carbonaceous chondrites** can be used as analogues to these asteroids (Wada et al., 2018; Schrader & Davidson, 2017).

Credits: Ryugu sample, JAXA

Meteorite Classification – Weissberg et al. (2006)

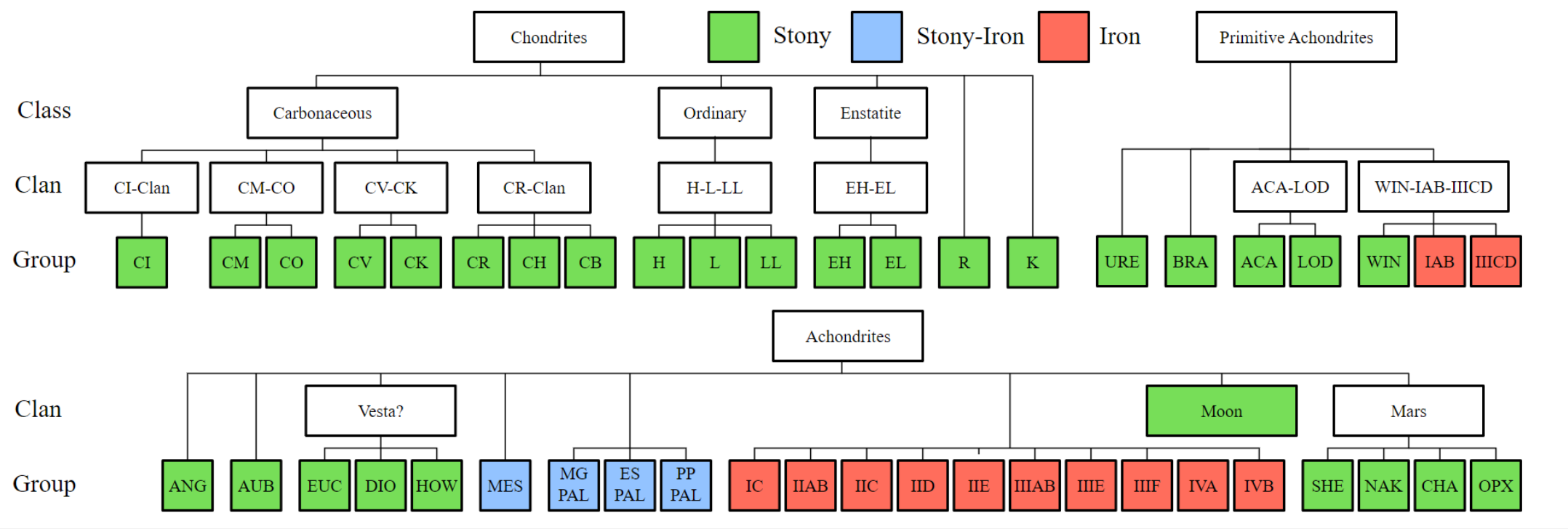

CAIs in CM Chondrites

- Carbonaceous chondrites are amongst the most studied meteorite samples; however, their origin and the evolution of their parent body(-ies) remains poorly understood.

- CM chondrites display **varying degrees of aqueous alteration**, spanning from 2.0–3.0 according to Rubin's scale.

- **Refractory inclusions** are the first solids to have formed in the Solar System and have witnessed:
  - **Thermal alteration** (e.g. annealing) prior to incorporation in CM parent body
  - **Fluid alteration events** after accretion

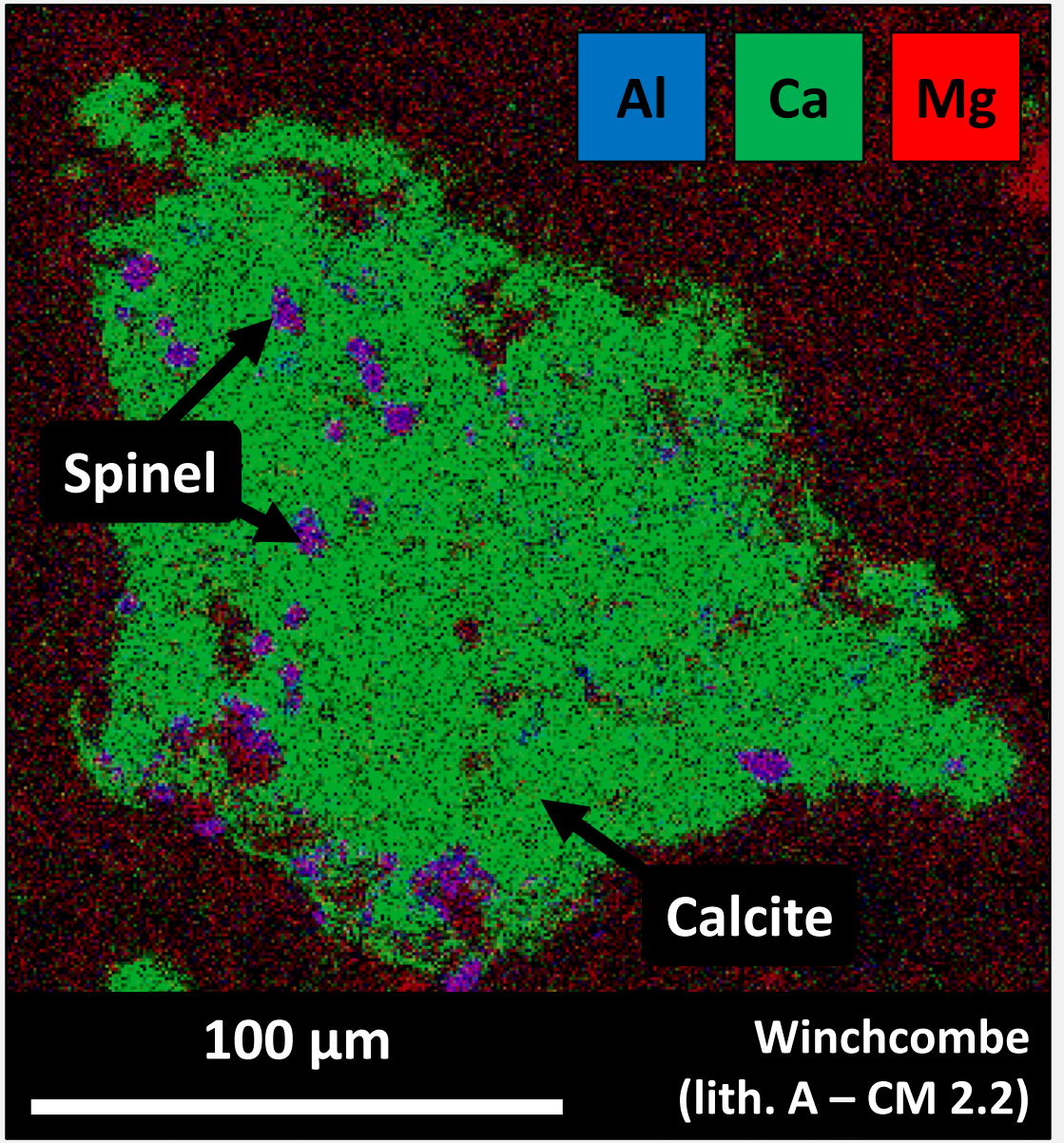

CM Classification – Rubin (2015)

Petrologic subtype	**2.7**	**2.6**	**2.5**	**2.4**	**2.3**	**2.2**	**2.1**	**2.0**
Chondrule mesostases	Phyllosilicate	Phyllosilicate	Phyllosilicate	Phyllosilicate	Phyllosilicate	Phyllosilicate	Phyllosilicate	Phyllosilicate
Matrix phyllosilicates	Abundant	Abundant	Abundant	Abundant	Abundant	Abundant	Abundant	Abundant
Matrix composition: MgO/"FeO"	0.35-0.43	0.35-0.43	0.35-0.43	0.35-0.43	0.50-0.70	0.50-0.70	0.50-0.70	0.50-0.70
Matrix composition: S/SiO_2	0.10-0.18	0.10-0.18	0.10-0.16	0.10-0.16	0.07-0.08	0.07-0.08	0.05-0.07	0.05-0.07
Metallic Fe-Ni (vol%)	1-2	~1	0.03-0.30	0.03-0.30	0.03-0.30	0.03-0.30	≤0.02	≤0.02
Mafic silicate phenocrysts in chondrules	Unaltered	Unaltered	Unaltered	Unaltered	2-15% altered	15-85% altered	85-99% altered	Completely altered
Large TCI clumps (vol%)	5-20	15-40	15-40	15-40	15-40	15-40	2-5	2-5
TCI composition: "FeO"/SiO2	4.0-7.0	2.0-3.3	2.0-3.3	1.5-2.0	1.5-2.0	1.0-1.7	1.0-1.7	1.0-1.7
TCI composition: S/SiO_2	0.40-0.60	0.18-0.35	0.18-0.35	0.14-0.20	0.14-0.20	0.05-0.09	0.05-0.09	0.05-0.09
Sulphide	po + pn	Mainly po + pn	Mainly po + pn	po + pn + int	po + pn + int	Mainly pn + int	Mainly pn + int	Mainly pn + int
Carbonate	Ca carbonate	Ca carbonate	Ca carbonate	Ca carbonate	Ca carbonate	Ca carbonate	Ca carbonate and complex carbonate	Ca carbonate and complex carbonate

Doctoral Research Outline

Classification and study of CAI populations within CMs

Aqueous alteration effects recorded within CM CAIs

Origin of Compound-Chondrule-CAIs within CMs

Doctoral Research – 1

Classification and study of CAI populations within CMs

- **Classification of CAIs within CMs**
- **Distribution of CAI types**
- **CAI modal abundances**
- **Sample-wide SEM + EDS analyses**

Aqueous alteration effects recorded within CM CAIs

Origin of Compound-Chondrule-CAIs within CMs

CAI Identification

CAI Identification

- Scanning Electron Microscopy
- Energy-Dispersive X-ray Spectroscopy

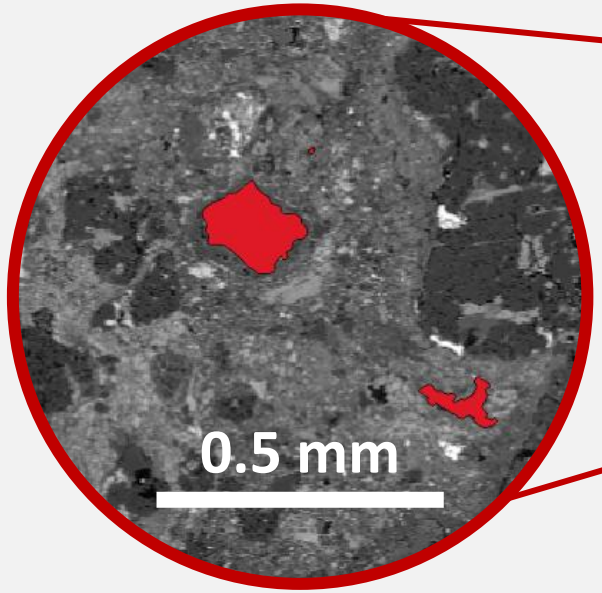

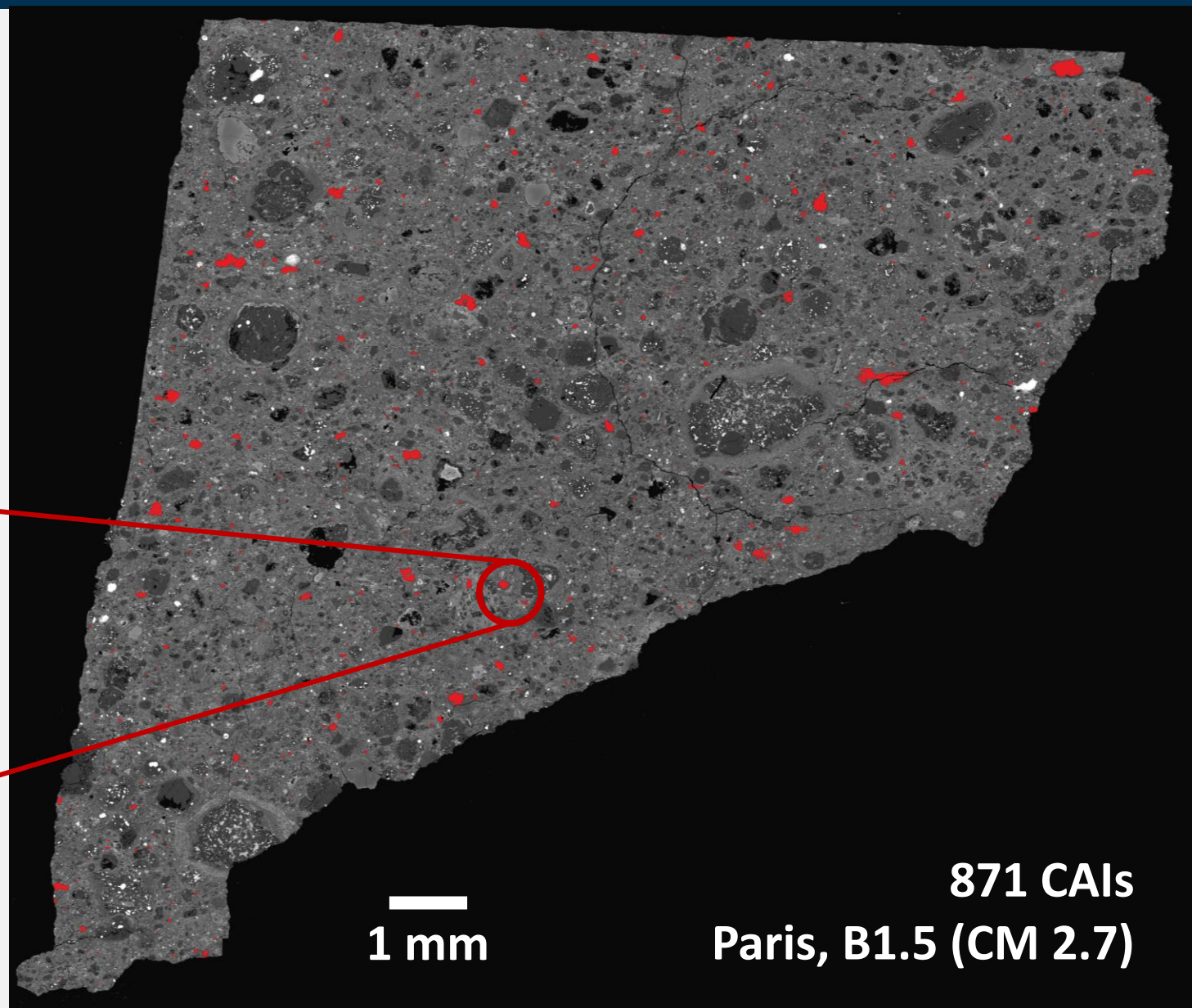

CAI Identification

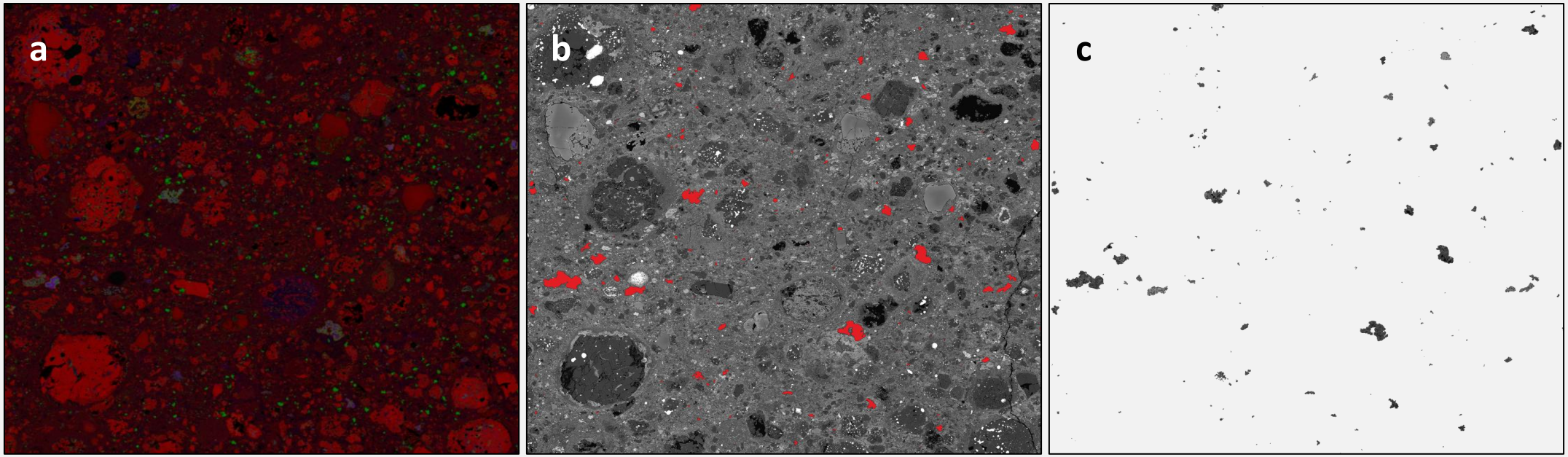

Al Ca Mg

Paris, B1.5 (CM2.7)

2.5 mm

2D CAI Measurements

- **CAI areas** were measured using *ImageJ* (**true**) and calculated (**calc.**) to be made comparable with existing literature:

$$area_{CAI\ calc.} = L \times S$$

- **CAI sizes** were reported as both "**true**" and **calculated** mean apparent diameters:

$$d_{CAI\ true} = 2 \times \sqrt{\frac{area_{CAI\ true}}{\pi}} \qquad d_{CAI\ calc.} = \frac{L \times S}{2}$$

- **CAI modal abundances** were expressed as described by Hezel et al. (2008):

$$A_{CAI} = \frac{\sum area_{CAIs}}{\sum area_{samples}}$$

CAI Modal Abundances in CM Chondrites

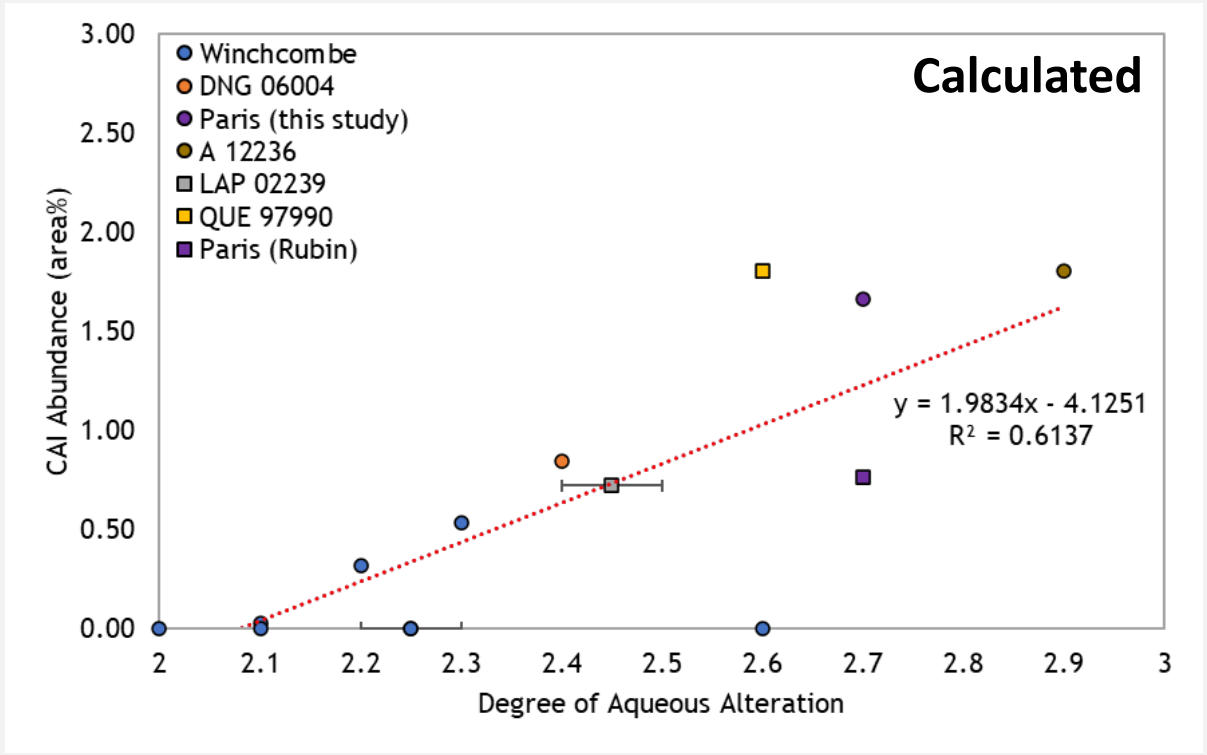

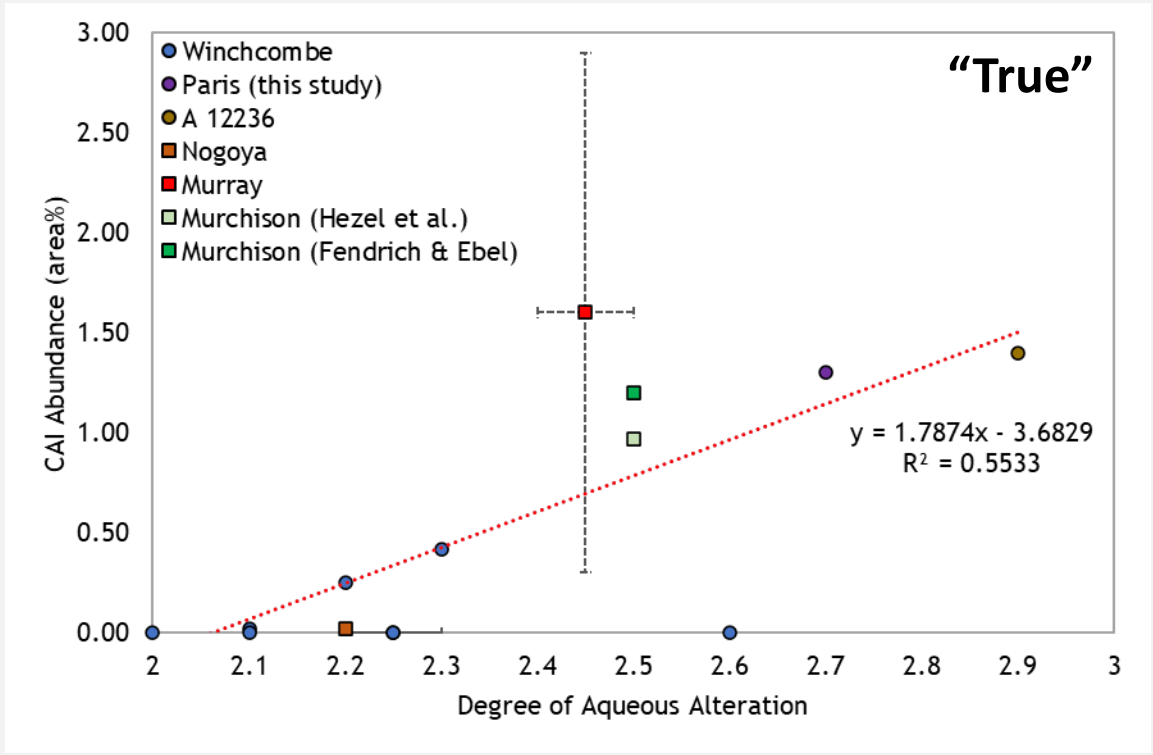

Doctoral Research – 2

Classification and study of CAI populations within CMs

Aqueous alteration effects recorded within CM CAIs

Origin of Compound-Chondrule-CAIs within CMs

- Pre- and post-accretionary histories of CAIs in Winchcombe
- Sample-wide SEM + EDS analyses
- Electron Probe Micro-Analysis (EPMA) of CAI refractory phases
- FIB-TEM + Transmission Kikuchi Diffraction (TKD) of section of CAI

The case of the Winchcombe Meteorite

#	Section ID	Lithology	Type	Mineralogy	FGR
1	P30540	Mx	Simple incl.	Sp-Phyll	Complete
2	P30542	B	Simple incl.	Ol-Sp-Pv-Phyll	Incomplete
3	P30545	Mx	Simple incl.	Sp-Px-Pv	Complete
4	P30545	Mx	Simple incl.	Sp-Px	Incomplete
5	P30545	B	Simple incl.	Sp-Ol	Complete
6	P30547	Mx	Simple agg.	Sp-Ol	Incomplete
7	P30547	Mx	Simple agg.	Px-Sp	Complete
8	P30547	Mx	Simple agg.	Sp-Ol-Hb-Pv	Absent
9	P30547	Mx	Complex agg.	Cal-Sp-Px-Ol-Pv	Complete
10	P30547	Mx	Simple incl.	Ol-Phyll-Sp-Pv	Incomplete
11	P30548	E	Simple incl.	Phyll-Sp	Complete
12	P30548	E	Simple agg.	Sp-Px-Phyll	Incomplete
13	P30549	FC	Simple agg.	Ol-Px-Sp-Pv	Absent
14	P30549	FC	Simple agg.	Ol-Px-Sp-Pv	Absent
15	P30552	A	Complex agg.	Cal-Px-Pv	Incomplete
16	P30552	A	Simple incl.	Sp-Px-Ol	Complete
17	P30552	A	Simple incl.	Cal-Px-Ol-Sp	Complete
18	P30552	A	Simple incl.	Cal-Ol-Sp	Incomplete
19	P30552	A	Complex agg.	Cal-Px-Sp-Pv-Gro	Complete
20	P30555	A	Simple incl.	Cal-Sp-Px-Arg	Complete
21	P30555	A	Simple incl.	Cal-Pv-Sp-Px	Complete

Credits: Àine O'Brien

Winchcombe CAI Populations

#	Section ID	Lithology	Type	Mineralogy	FGR
1	P30540	Mx	Simple incl.	Sp-Phyll	Complete
2	P30542	B	Simple incl.	Ol-Sp-Pv-Phyll	Incomplete
3	P30545	Mx	Simple incl.	Sp-Px-Pv	Complete
4	P30545	Mx	Simple incl.	Sp-Px	Incomplete
5	P30545	B	Simple incl.	Sp-Ol	Complete
6	P30547	Mx	Simple agg.	Sp-Ol	Incomplete
7	P30547	Mx	Simple agg.	Px-Sp	Complete
8	P30547	Mx	Simple agg.	Sp-Ol-Hb-Pv	Absent
9	P30547	Mx	Complex agg.	Cal-Sp-Px-Ol-Pv	Complete
10	P30547	Mx	Simple incl.	Ol-Phyll-Sp-Pv	Incomplete
11	P30548	E	Simple incl.	Phyll-Sp	Complete
12	P30548	E	Simple agg.	Sp-Px-Phyll	Incomplete
13	P30549	FC	Simple agg.	Ol-Px-Sp-Pv	Absent
14	P30549	FC	Simple agg.	Ol-Px-Sp-Pv	Absent
15	P30552	A	Complex agg.	Cal-Px-Pv	Incomplete
16	P30552	A	Simple incl.	Sp-Px-Ol	Complete
17	P30552	A	Simple incl.	Cal-Px-Ol-Sp	Complete
18	P30552	A	Simple incl.	Cal-Ol-Sp	Incomplete
19	P30552	A	Complex agg.	Cal-Px-Sp-Pv-Gro	Complete
20	P30555	A	Simple incl.	Cal-Sp-Px-Arg	Complete
21	P30555	A	Simple incl.	Cal-Pv-Sp-Px	Complete

- TCI-like objects and Mg-Fe serpentine have been reported to replace Ca-carbonates in Winchcombe's matrix, including type 1 calcite.
- No calcite within the CAIs can be seen being replaced or rimmed by TCI/serpentine. The calcite in the calcitised CAIs is likely type 2b, as it is polycrystalline, presents microporosities, and is not rimmed by tochilinite/serpentine.
- This suggests that type 2 calcite precipitated after the formation of TCI/serpentine as there is no calcite replacement by TCI/serpentine in the CAIs observed.

Secondary Mineralisation Events Recorded in CAIs

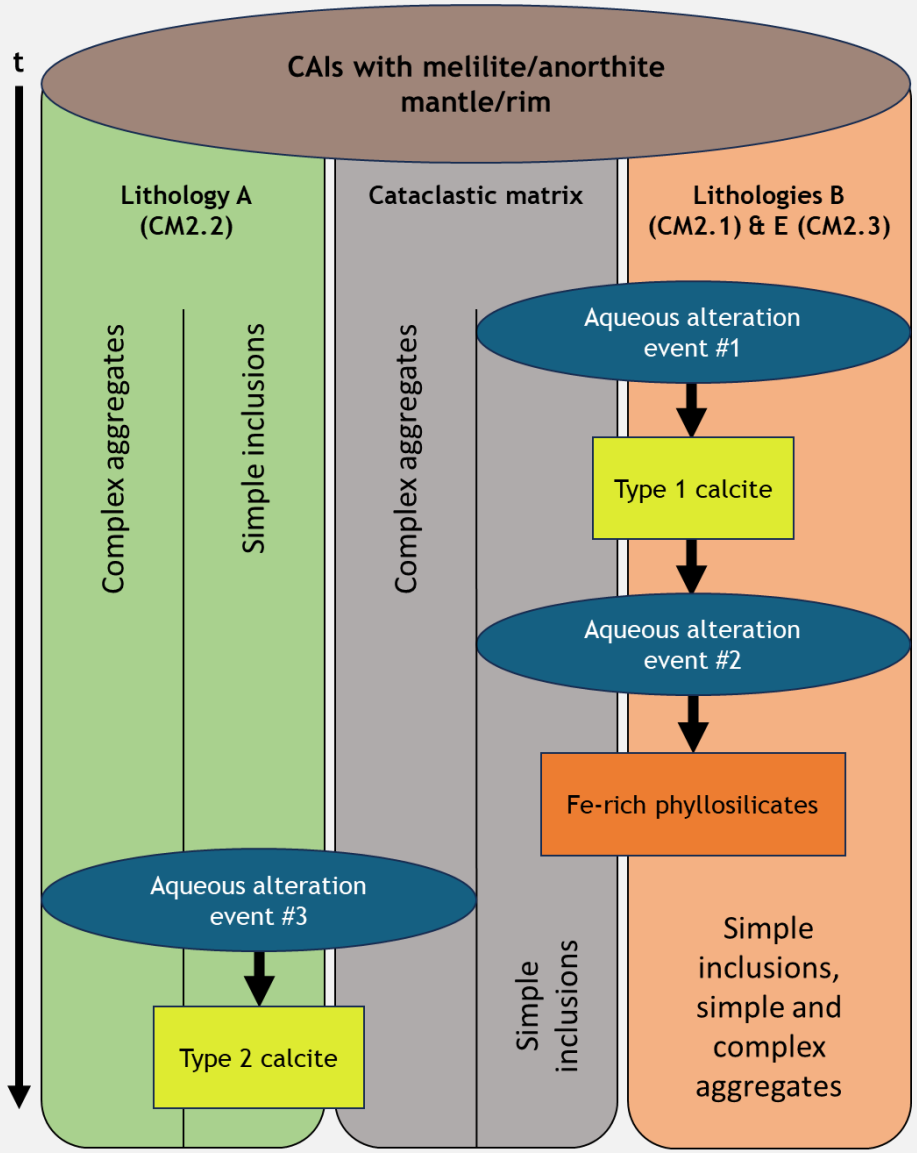

1) Simple inclusions and aggregates from lith. E, along with a few simple inclusions from lith. B and Mx, that experienced an early fluid-driven replacement of melilite/anorthite by type 1 calcite, before undergoing a second alteration event, leading to the replacement of said-calcite with Fe-rich phyllosilicates.

2) Complex aggregates and several simple inclusions from lith. A, along complex aggregates from Mx that underwent a later alteration event, replacing their melilite/anorthite mantles/rims with type 2 calcite.

3) The rest of the simple inclusions and aggregates from lithologies A, B, FC, and Mx that did not visibly experience the described alteration events.

Doctoral Research – 3

Classification and study of CAI populations within CMs

Aqueous alteration effects recorded within CM CAIs

Origin of Compound-Chondrule-CAIs within CMs

- Description and study of CCCAIs
- Sample-wide SEM + EDS analyses
- Electron Backscatter Diffraction (EBSD) analyses of CCCAIs
- Secondary Ion Mass Spectrometry (SIMS) on CAIs and chondrules

CCCAIs in CM Chondrites

- **Compound-Chondrule-Calcium-Aluminium-rich Inclusions** (CCCAIs) have been described as either CAIs enclosing chondrules or **chondrules enclosing CAIs**.
- **Rare occurrences**, although previously reported within most major carbon-aceous groups (CO, CV, and CH).
- The existence of CCCAIs suggests that **chondrules and CAIs interacted within high-particle-density environments** in the protoplanetary disk prior to their incorporation into their mutual parent bodies.

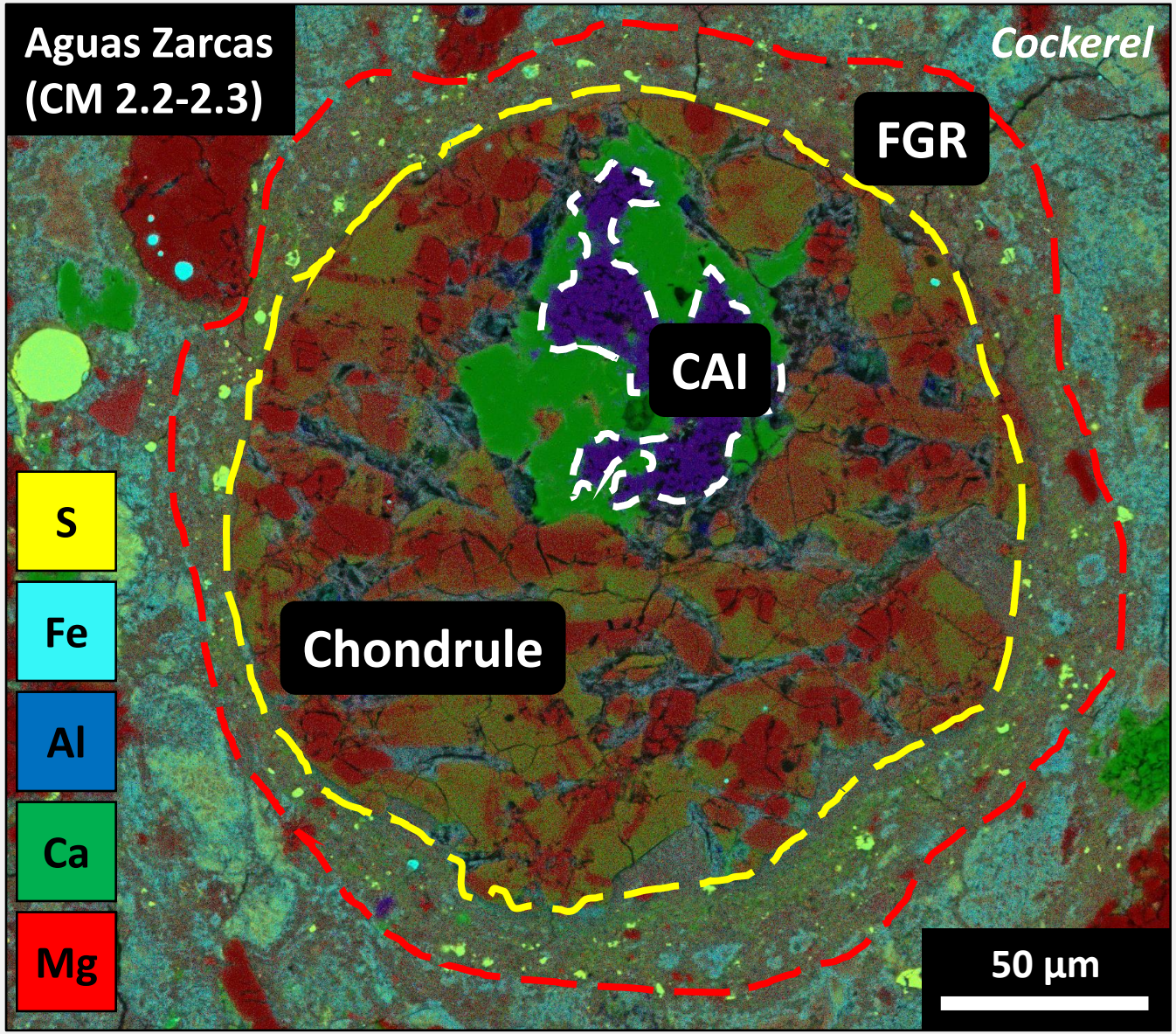

EBSD Phase Map of the Cockerel

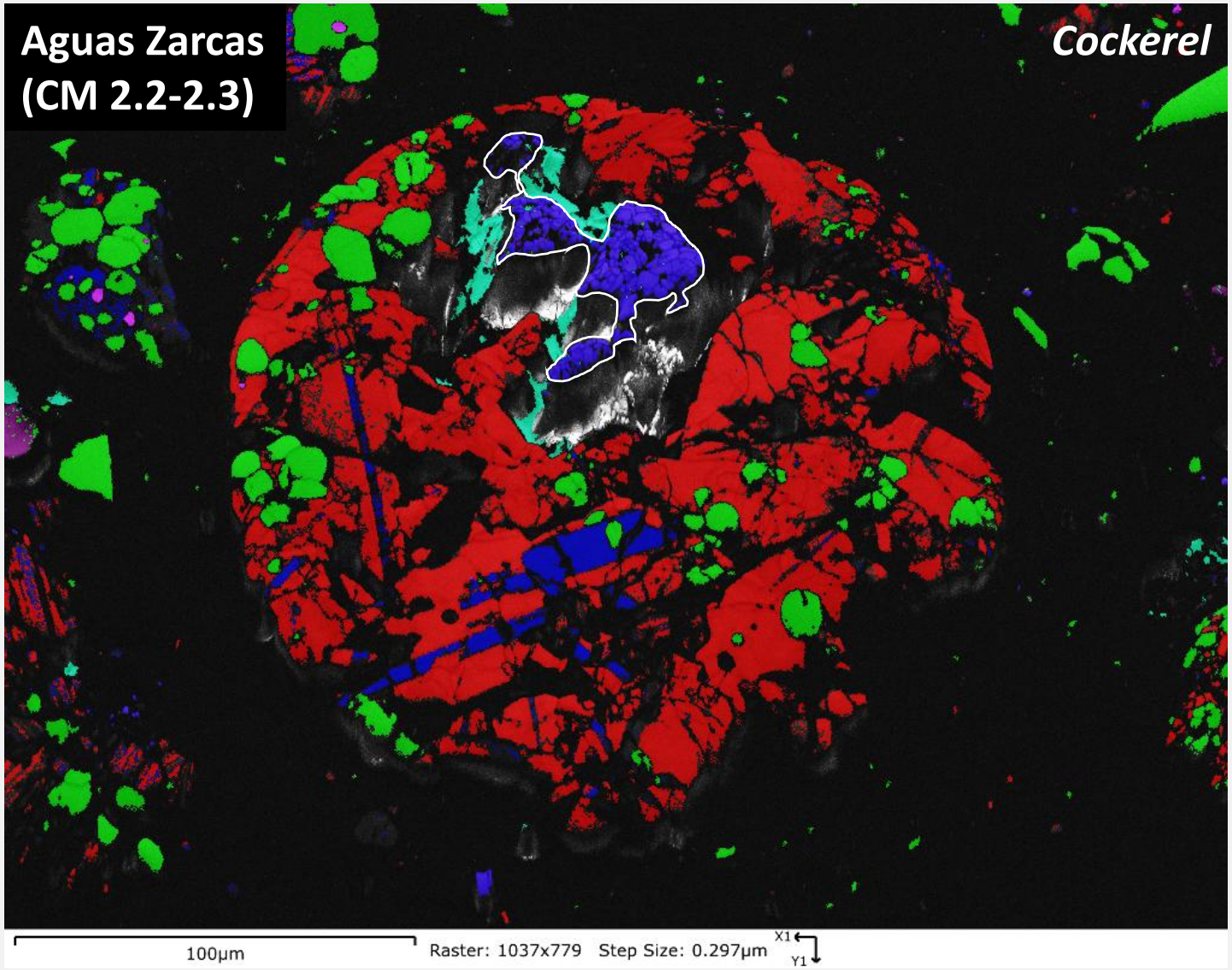

Diopside

Forsterite

Spinel

Enstatite

Calcite

Proposed Model for the Formation of CCCAIs

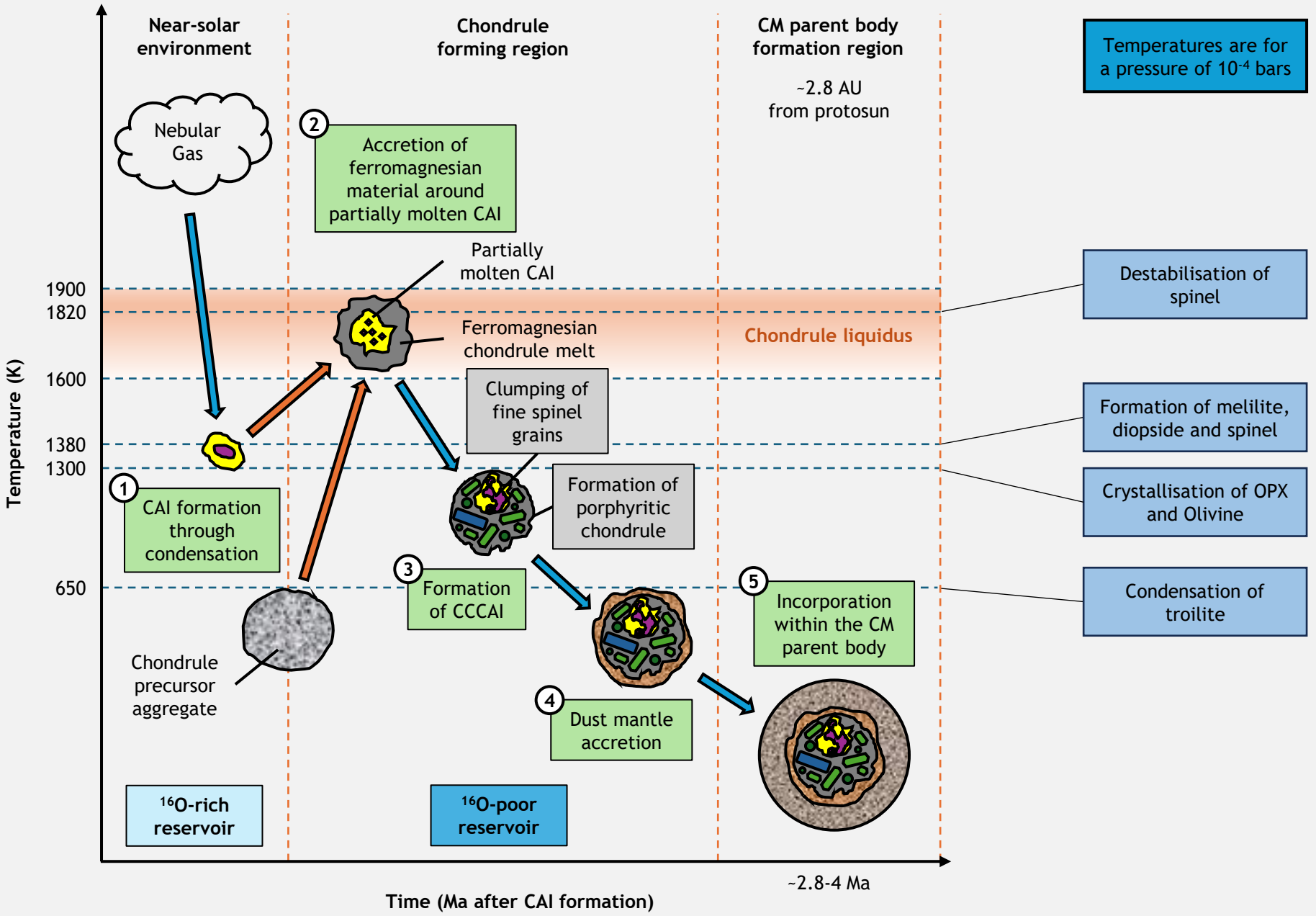

Key Findings

- **CM CAI modal abundance decreases relative to increasing aqueous alteration** due to the alteration and destruction of CAIs through fluid-mediated replacement reactions. This correlation may serve as an additional criterion for determining the degree of aqueous alteration in CM chondritic lithologies.

- **Initial distribution of CAIs within the CM parent body(-ies) was likely homogeneous**, and heterogeneity in the CAI record was caused by subsequent occurring fluid-driven alteration events.

- Lithological heterogeneity within CM samples must be considered, as the **CM parent body(-ies) underwent heterogeneous aqueous alteration.**

- **CCCAIs are rare objects within CM chondrites** and are formed by the incorporation of CAIs within a precursor ferromagnesian melt during transient heating events in the chondrule forming region.

- The **existence of CCCAIs evidences an early outward migration of near-solar refractory material** within 1 Ma after CAI formation (before the formation of a physical barrier, e.g. proto-Jupiter).

Searching for Micron- to Sub-micron-sized Glassy and C-rich Phases in Martian and Carbonaceous Meteorites

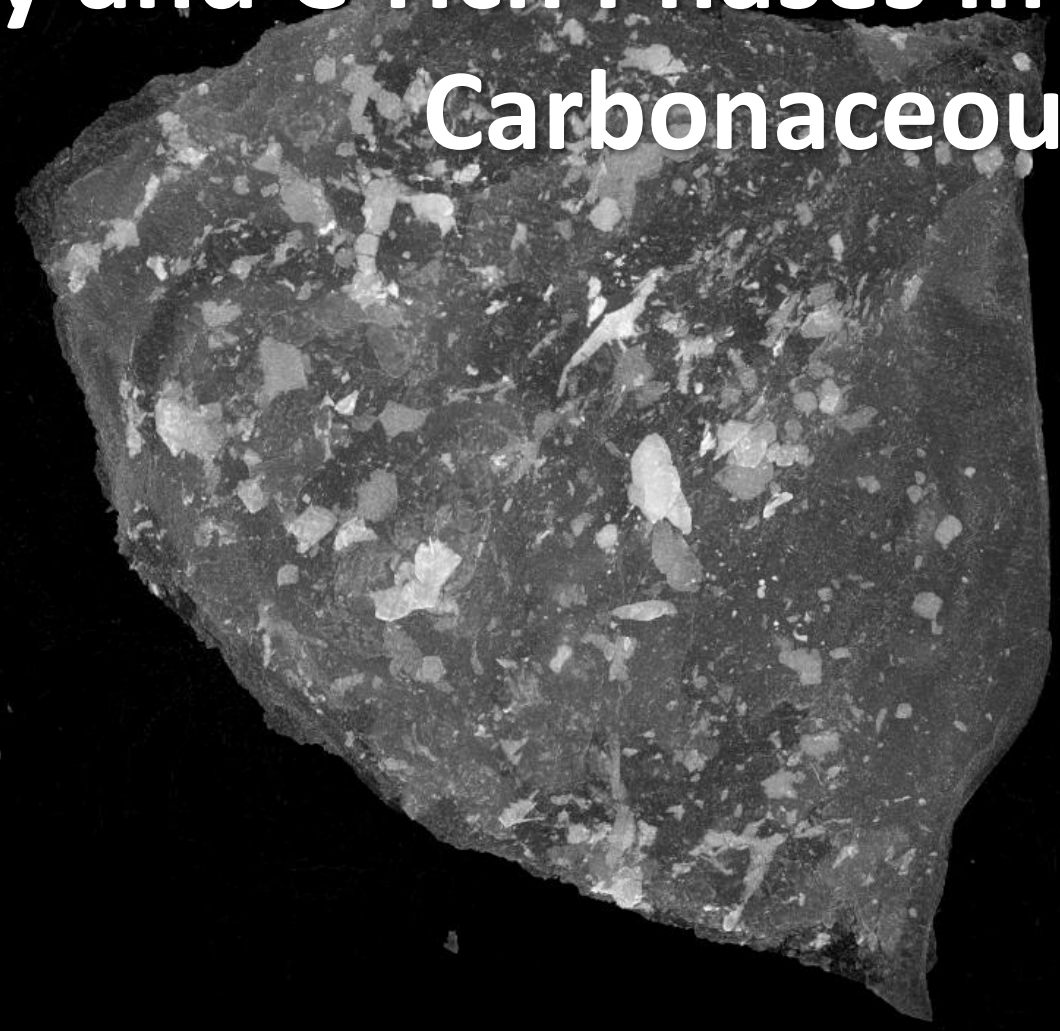

Maximum Intensity Projection (MIP) of a chip of Tissint (ETH-10) obtained at the Institute of Anatomy (University of Bern, Switzerland) using nano-XCT (400 nm per voxel size).

Searching for C-rich Nanoglobules in C-type Chondrites

- **Nanoglobules** are microscopic, hollow (seldom solid), spherical to irregular organic-rich grains (De Gregorio, 2015). These globules can range from a few 100s of nm to 2 microns in diameter (Mathurin et al., 2024).

- The densities of these nanoglobules would be low compared to their surrounding phases, similar to other **organic matter** in **carbonaceous meteorites**, due to their composition (e.g. C, O, N, and S).

- Sub-mm carbonaceous meteorite samples (CMs and CIs) were selected as analogues for samples from asteroids Ryugu and Bennu.

Searching for Glassy Inclusions in Martian Meteorites

- In the **Martian meteorites**, the aim is to be able to resolve sub-mm, down to a few micron-wide **glass veins and beads** (Wiens et al., 1985; Bogard and Garrison, 1998; Aoudjehane et al., 2005; Avice et al., 2018).

- **Glassy inclusions** found within Martian meteorites (i.e. shergottites) have provided insights into the composition and evolution of the **Martian atmosphere**, which remains poorly constrained (Wiens, 1986; Wiens et al., 1988).

- The densities of these glass inclusions should vary from 2.50 to 2.80 $g.cm^{-3}$. Basaltic (tholeiitic) glasses: ~2.78 $g.cm^{-3}$. Soil models use 2.55 $g.cm^{-3}$. Similar to feldspar and plagioclase (2.56-2.78 $g.cm^{-3}$), but distinct from Martian pyroxenes (3.2-3.45 $g.cm^{-3}$) and olivine (~3.3 $g.cm^{-3}$).

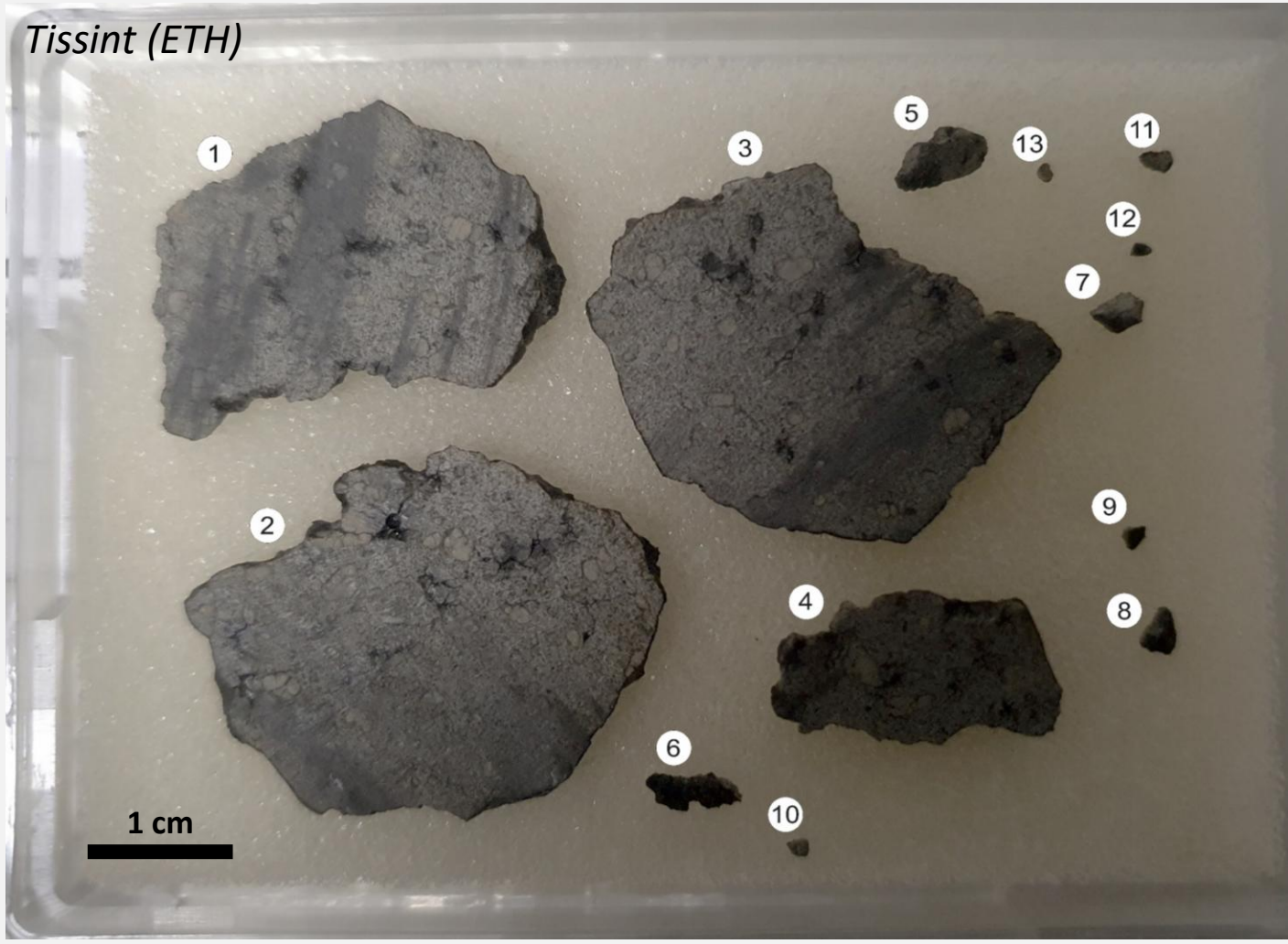

Aims & Objectives

Correlated approach to the characterisation of Martian glassy inclusions

- Development and optimisation of NIR spectral deconvolution to derive quantitative mineral compositions, and on correlating these datasets with new and existing nXCT scans.
- Initial targets include sub-micron-sized impact melt inclusions in Martian meteorites (e.g., glass pockets in shergottites) to better understand the Martian paleo-environment.
- Further optimisation of the instrumental parameters (e.g., contrast enhancement, sample holder design, and sample size) is underway to improve spatial resolution.

Aims & Objectives

Correlated approach to the characterisation of Martian glassy inclusions

Identification and characterisation of nanoglobules within C-type asteroid analogues

- The technique will be further refined to locate C-rich nanoglobules within pristine carbonaceous meteorites (CI and CM) and, once available, grains from asteroids Ryugu and Bennu (De Gregorio, 2015; Mathurin et al., 2024).
- The initial instrumental setup will be complemented by UV fluorescence spectroscopy at the MIC of the University of Bern for larger-scale investigation of nanoglobules. This phase will yield a publication describing an integrated non-destructive approach for identifying nanoglobule aggregates in rare carbonaceous materials.

Aims & Objectives

Correlated approach to the characterisation of Martian glassy inclusions

Identification and characterisation of nanoglobules within C-type asteroid analogues

Geochemical and isotopic analyses of targeted regions of interest

- Identified regions of interest will be targeted for noble gas analyses (particularly Ne), which may reveal valuable information about the paleo-environment and atmospheric evolution of Mars (Crowther et al., 2022; Wieler et al., 2016; Boggard et al., 1998).
- Identified nanoglobule aggregates will also be selected for noble gas analyses to provide insights into the nature of the organic-rich phases, as C-type asteroids have been found to contain prebiotic organic compounds and are thought to be prime candidates for delivering prebiotic organics to early Earth.

Analyses in Progress (28-01-2026)

Name	Designation	Type	Weight (g)	Size (mm)		nXCT analyses	IR	Vis.
				Length	Width			
Nakhla	BE 613	Nakhlite	0.4714	10.0	7.0	4 and 1.8 µm/voxel	Y	Y
Chassigny	BE 612	Chassignite	0.0104	3.5	3.3		Y	Y
NWA 16272	AF-3	Vesicular basalt	0.0618	5.9	3.6	2 µm/voxel	Y	Y
Tissint	ETH-9	Shergottite	0.0035	2.0	2.0	500 nm/voxel	Y	Y
	ETH-10		0.0016	1.0	1.5	400 nm/voxel	Y	Y
	ETH-12		0.0014	1.5	1.5	450 nm/voxel	Y	Y
	ETH-13		0.0017	2.0	1.0	500 nm/voxel	Y	Y
Cold Bokkeveld	BE 366-3	CM2.2	0.0051	3.2	2.1		Y	Y
Mighei	-	CM2.3	0.0024	1.7	1.3		Y	Y
Orgueil	No 219	CI1	0.0033	2.2	1.7	850 nm/voxel	Y	Y

Analyses in Progress (28-01-2026)

W.I.P.

Name	Designation	Type	Weight (g)	Size (mm)		nXCT analyses	IR	Vis.
				Length	Width			
Nakhla	BE 613	Nakhlite	0.4714	10.0	7.0	4 and 1.8 µm/voxel	Y	Y
Chassigny	BE 612	Chassignite	0.0104	3.5	3.3	February 2026	Y	Y
NWA 16272	AF-3	Vesicular basalt	0.0618	5.9	3.6	2 µm/voxel	Y	Y
Tissint	ETH-9	Shergottite	0.0035	2.0	2.0	500 nm/voxel	Y	Y
	ETH-10		0.0016	1.0	1.5	400 nm/voxel	Y	Y
	ETH-12		0.0014	1.5	1.5	450 nm/voxel	Y	Y
	ETH-13		0.0017	2.0	1.0	500 nm/voxel	Y	Y
Cold Bokkeveld	BE 366-3	CM2.2	0.0051	3.2	2.1	February 2026	Y	Y
Mighei	-	CM2.3	0.0024	1.7	1.3	February 2026	Y	Y
Orgueil	No 219	CI1	0.0033	2.2	1.7	850 nm/voxel	Y	Y

Nano-XCT Scan of a Chip of Nakhla (4 microns per voxel)

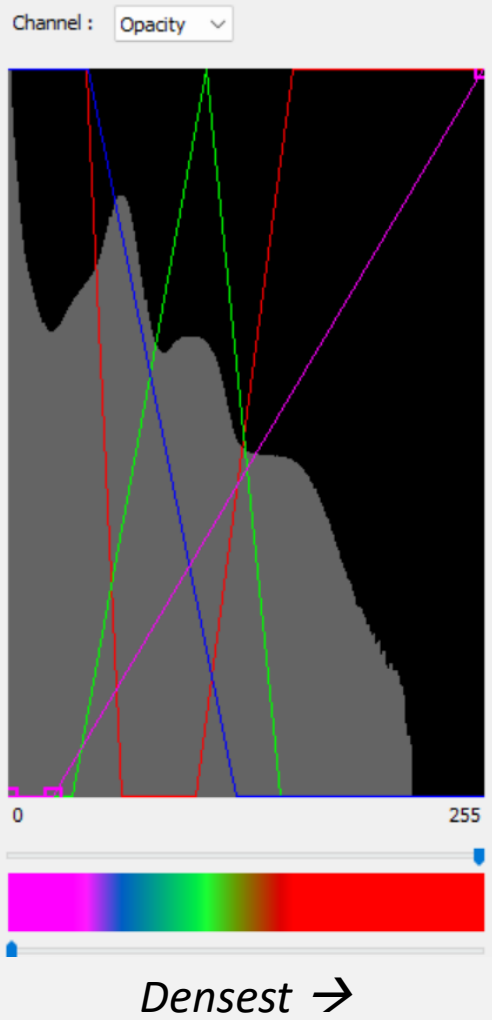

Densest →

- BE 613 Nakhla
  Helical acquisition
  100 kV
  Bruker SKYSCAN 2214
  Institute of Anatomy
- Sample was inserted into a slit in a piece of foam (invisible in XCT), which was closed with tape. The sample was never in contact with the tape.
- Specific sample holders for more precious samples can be 3D printed at the facility but must be individually designed.

Nano-XCT Scan of a Chip of Nakhla (4 microns per voxel)

87th Annual Meeting of the Meteoritical Society (14-18/07/2025)

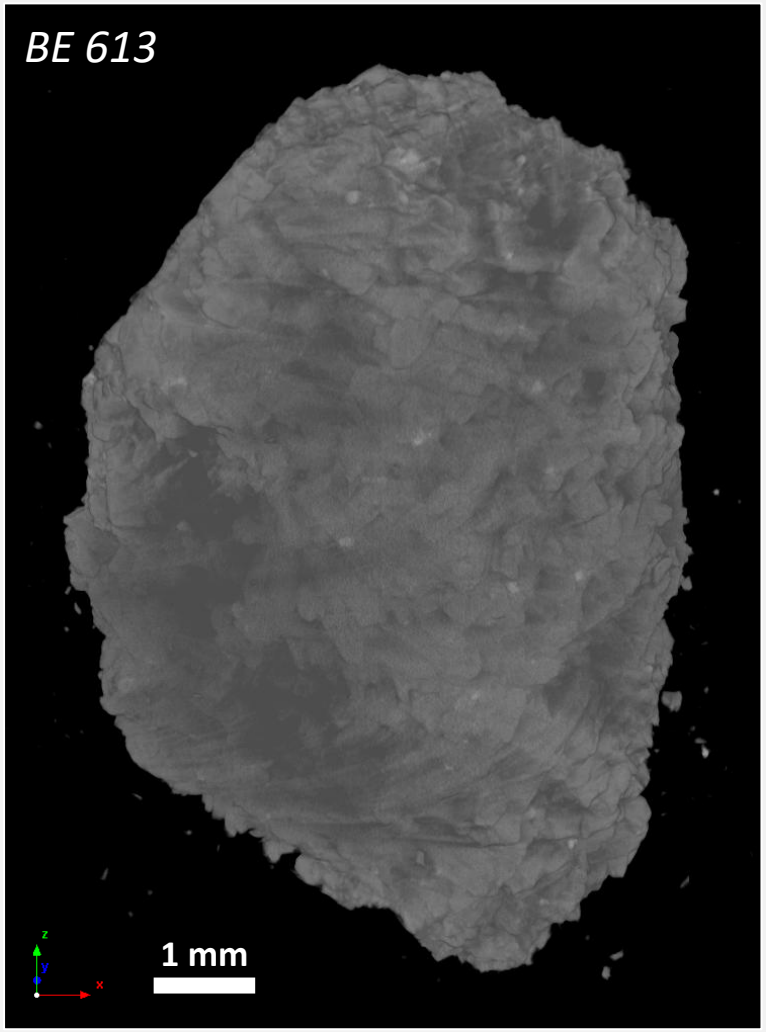

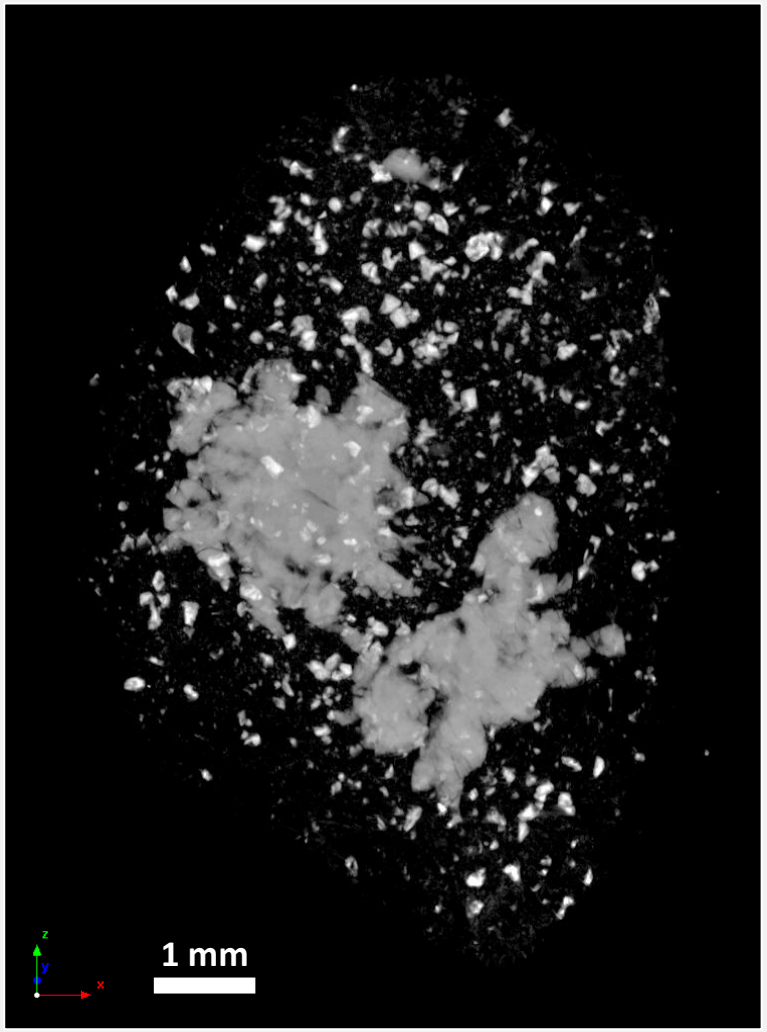

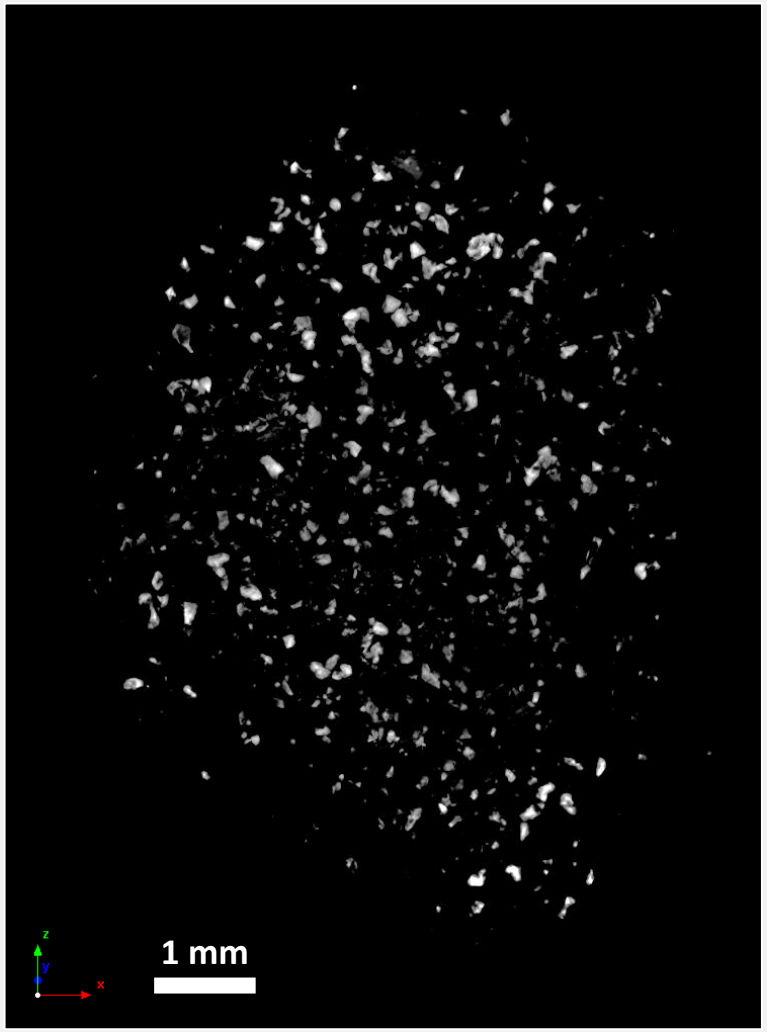

Nano-XCT Scan of a Chip of Nakhla (1.8 microns per voxel)

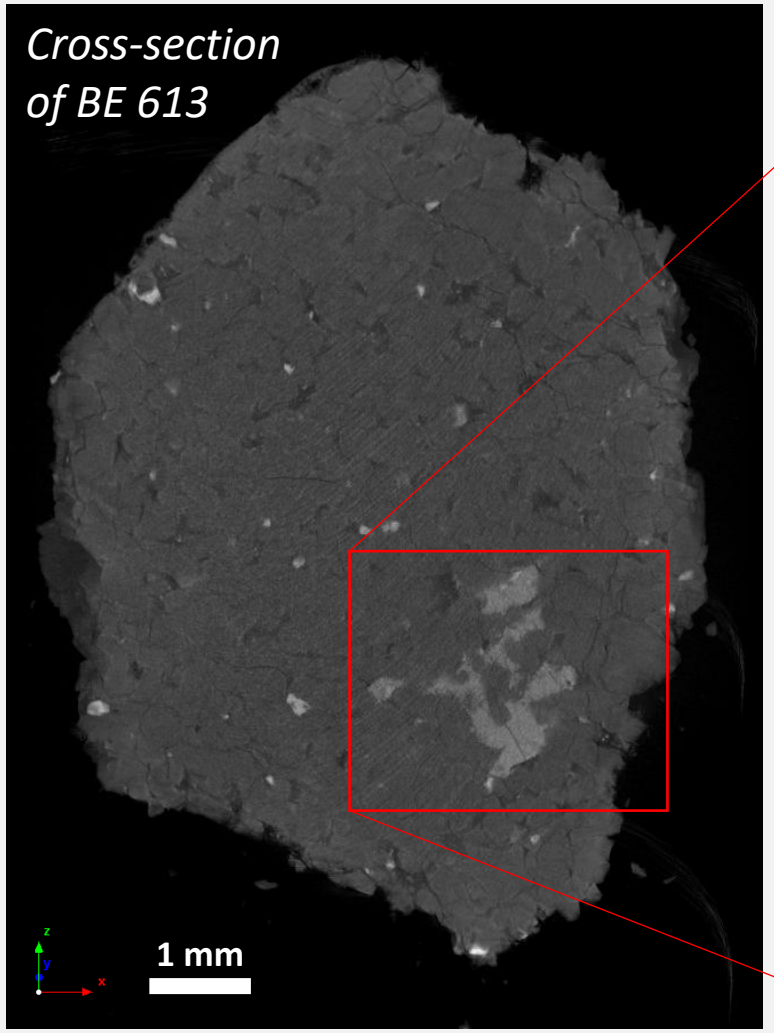

Nano-XCT Measurement Optimisation

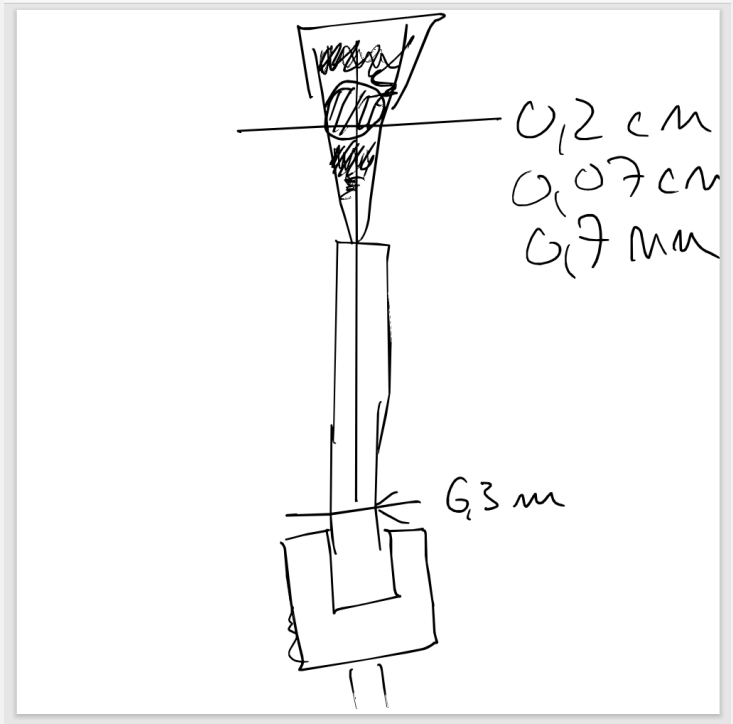

Dr. Haberthür
Institute of Anatomy

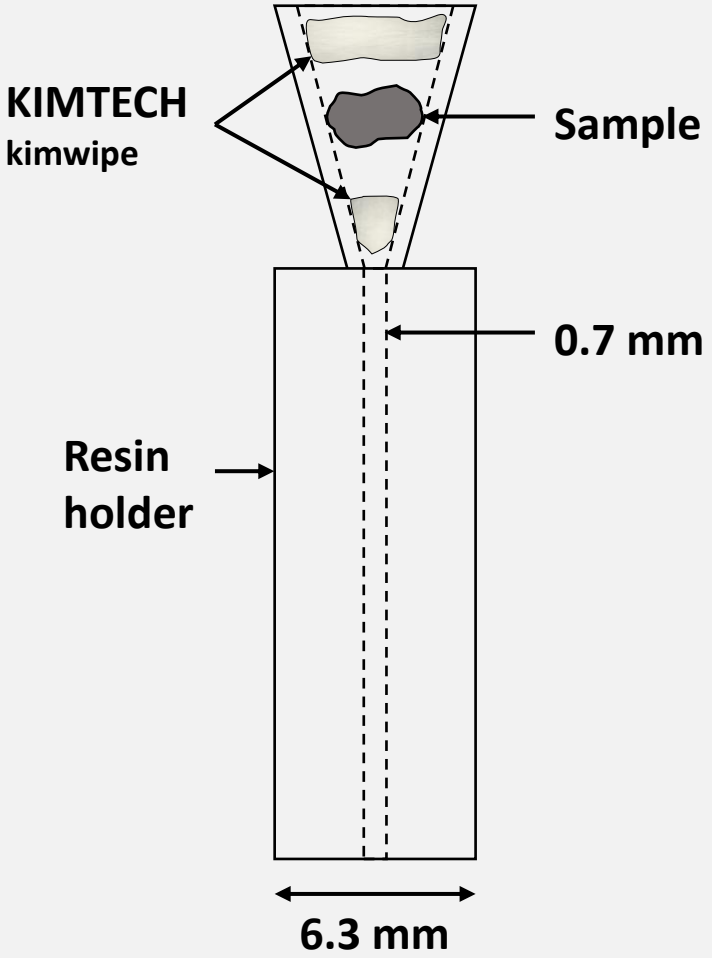

Nano-XCT Scan of a Chip of Tissint (400 nm per voxel)

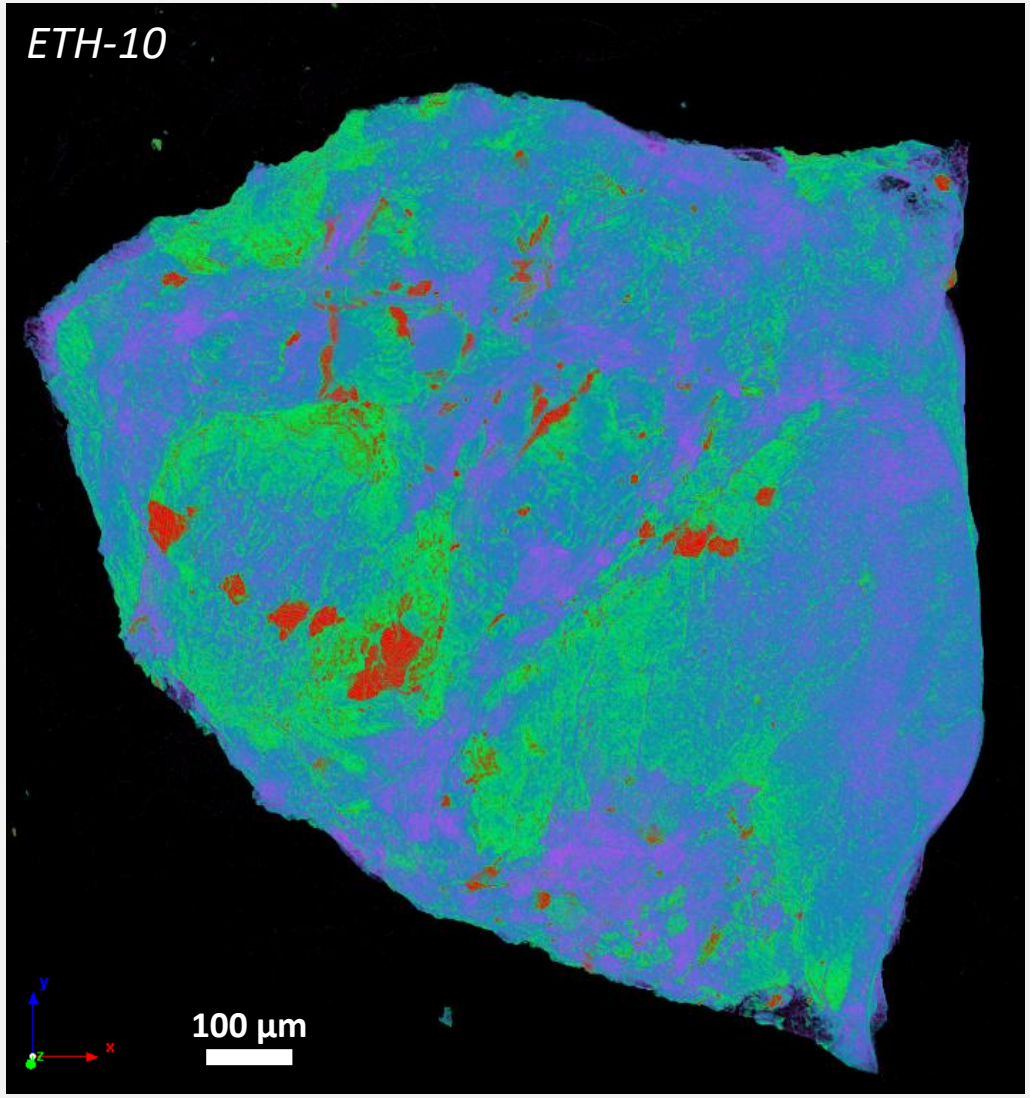

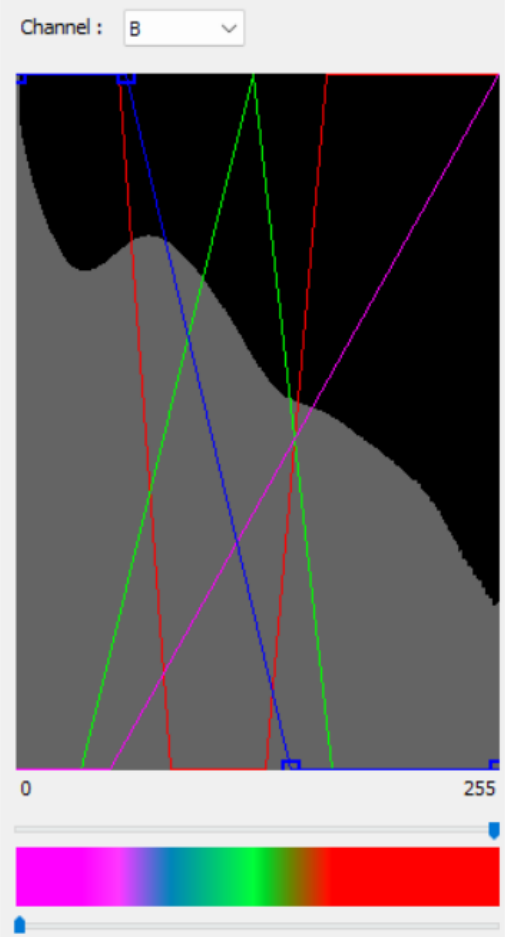

Densest →

- ETH-10 Tissint
  360° rotation
  80 kV
  Bruker SKYSCAN 2214
  Institute of Anatomy
- Analysed whilst within a specifically designed 3D-printed sample holder

W.I.P.

Nano-XCT Scan of a Chip of Tissint (450 nm per voxel)

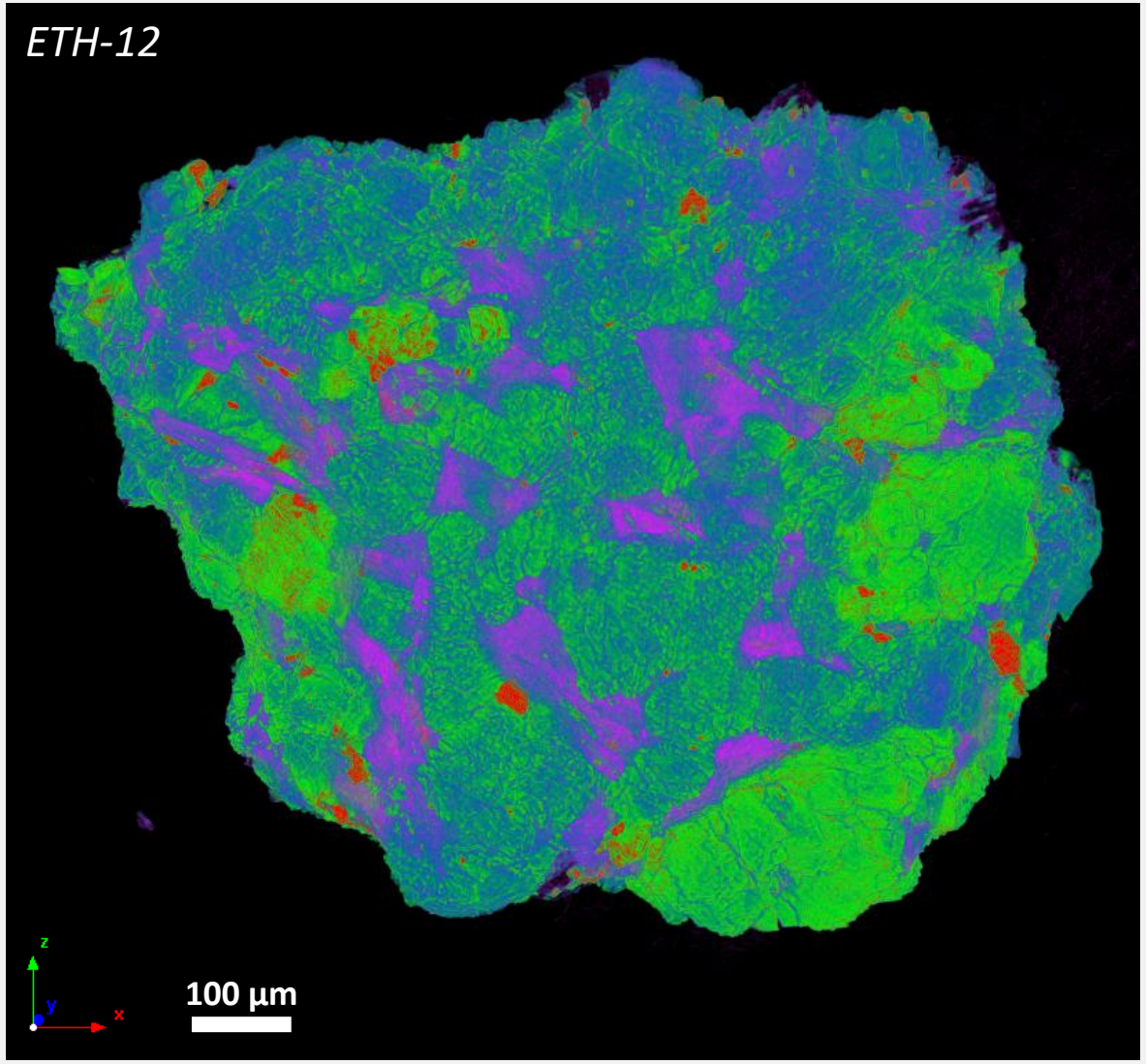

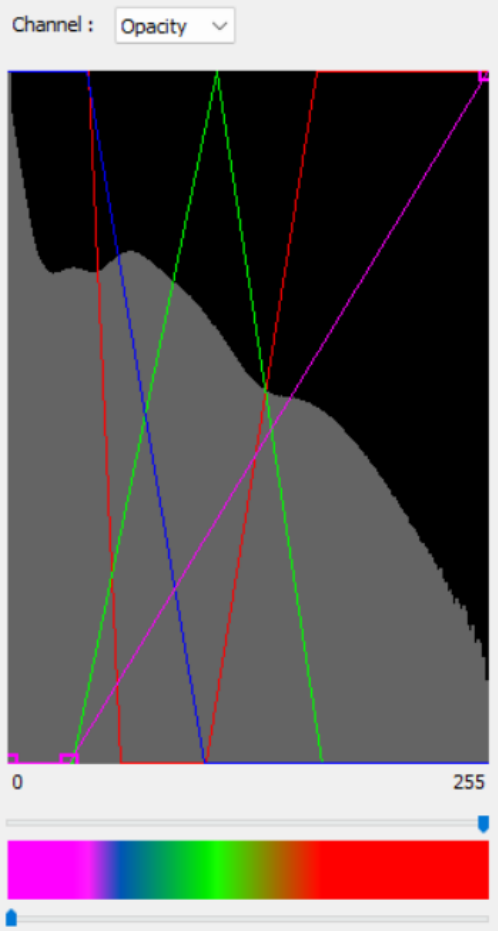

Densest →

- ETH-12 Tissint
  360° rotation
  80 kV
  Bruker SKYSCAN 2214
  Institute of Anatomy
- Analysed whilst within a specifically designed 3D-printed sample holder

W.I.P.

Reflectance Spectroscopy Optimisation

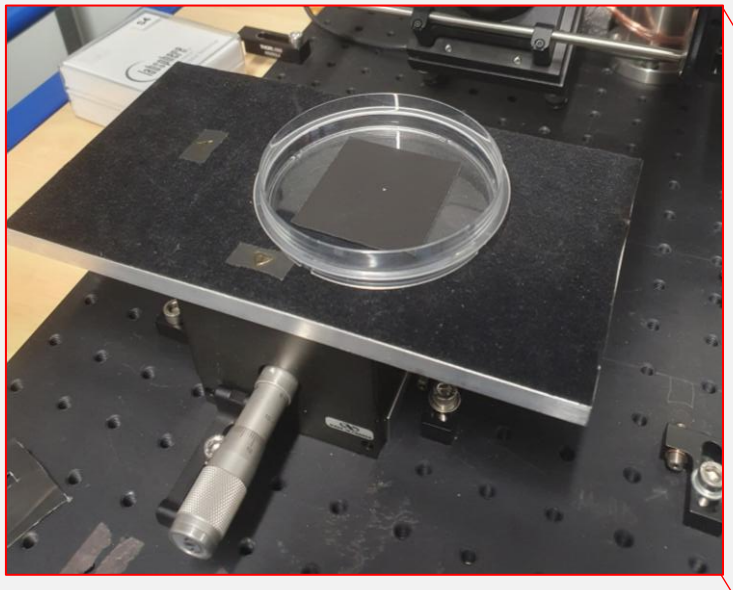

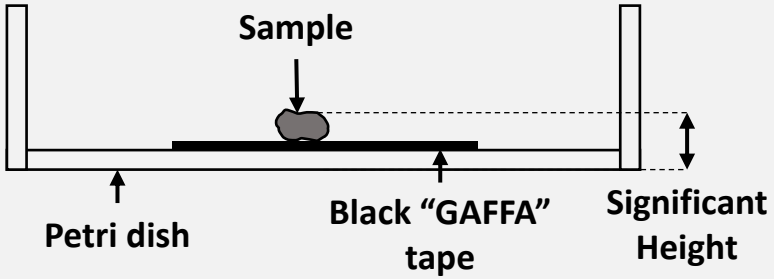

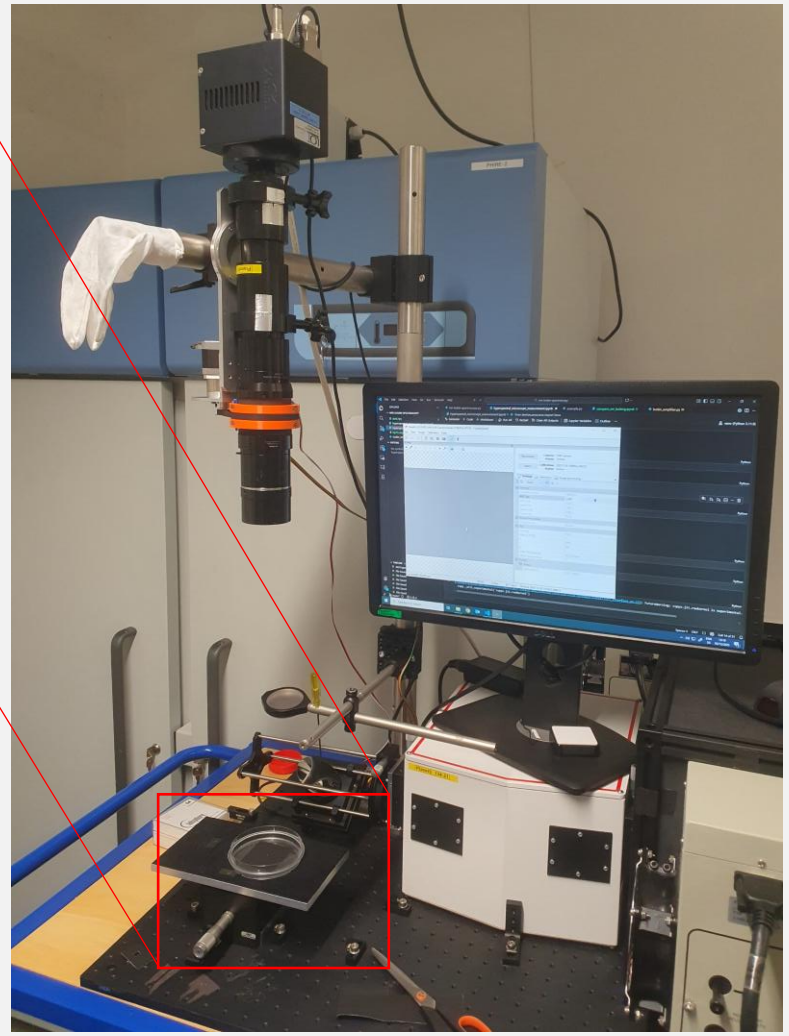

Absorption bands of the minerals of interest (400 to 2500 nm)

- Pyroxenes (~1-2 µm)
- Olivine (~0.7-1.8 µm, centred around ~1 µm)
- Plagioclase (0.8–1.7 µm, centred around ~1.1–1.3 µm)
- Carbonates (0.4-3 µm)
- Sulfates (~2.1-2.7 µm)

NIR and visible reflectance measurements made separately.

NWA 16272, AF-3 – A Martian Vesicular Basalt

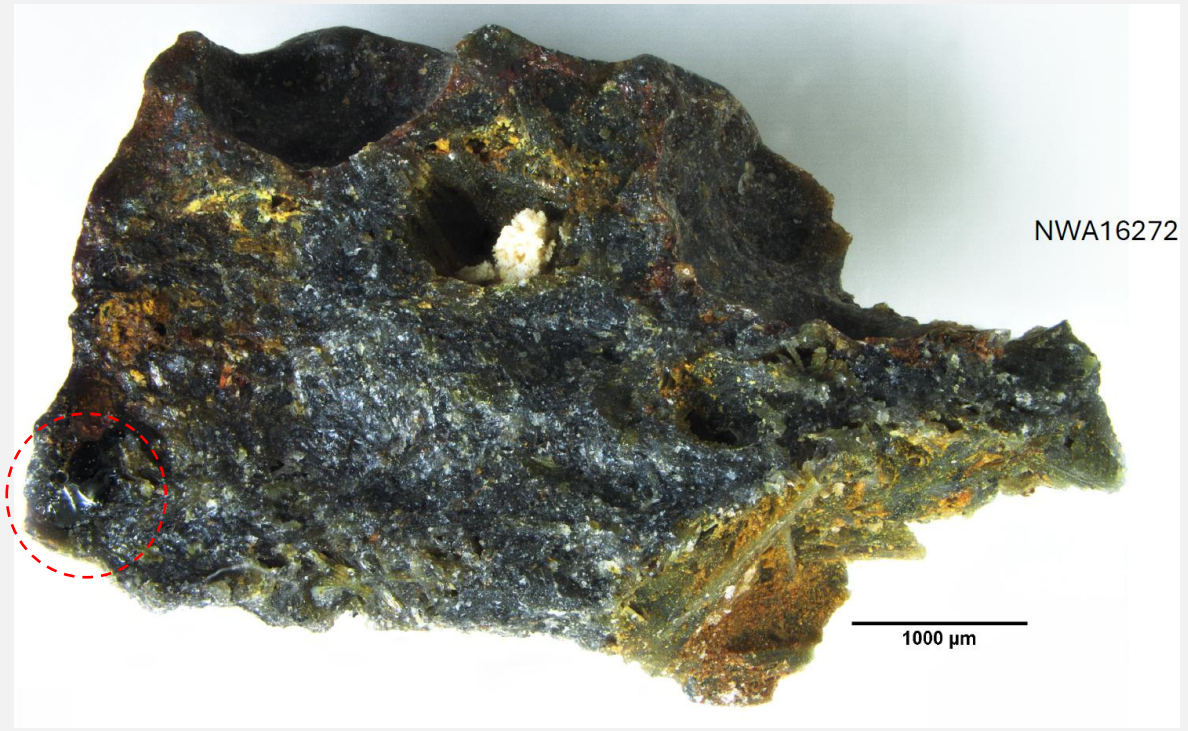

Prof. Busemann
ETH Zurich

Nano-XCT Scan of NWA 16272, AF-3 (2µm per voxel)

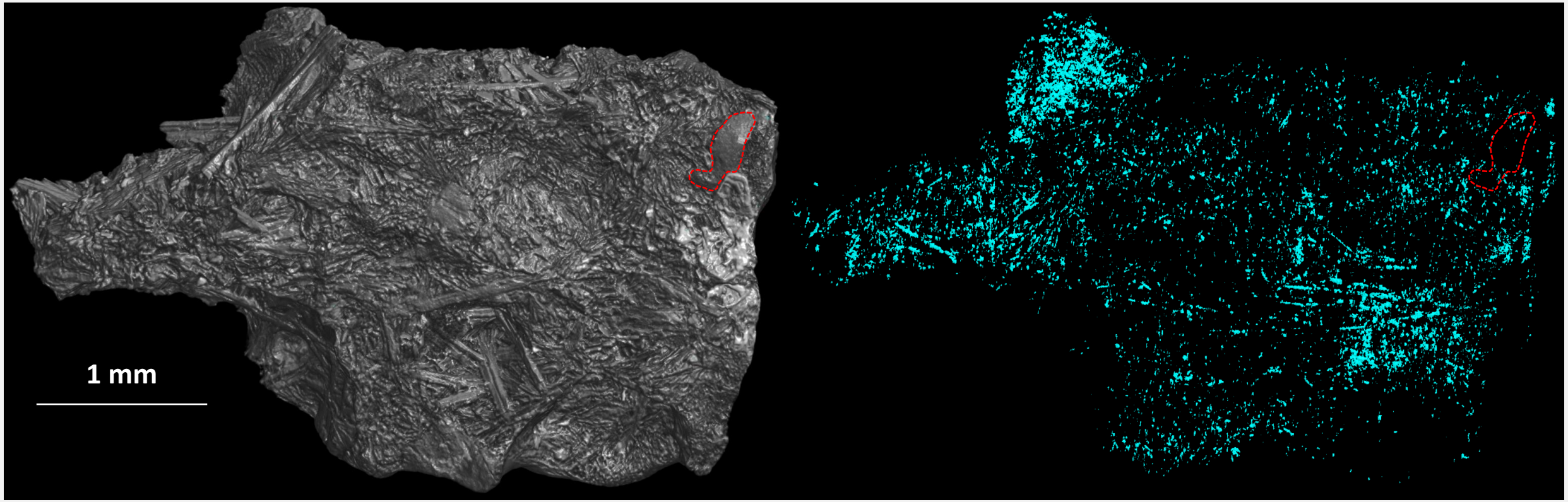

- ETH-12 Tissint
  360° rotation
  60 kV
  Bruker SKYSCAN 2214
  Institute of Anatomy

- Brighter phases correspond to minerals with higher X-ray absorption capacity which indicates a higher density.
- Identified glassy inclusion is outlined in red dashed lines.
- Internal porosity segmented using the model developed by Taute, C. et al. (2021)

Reflectance Spectra of NWA 16272, AF-3 (face A)

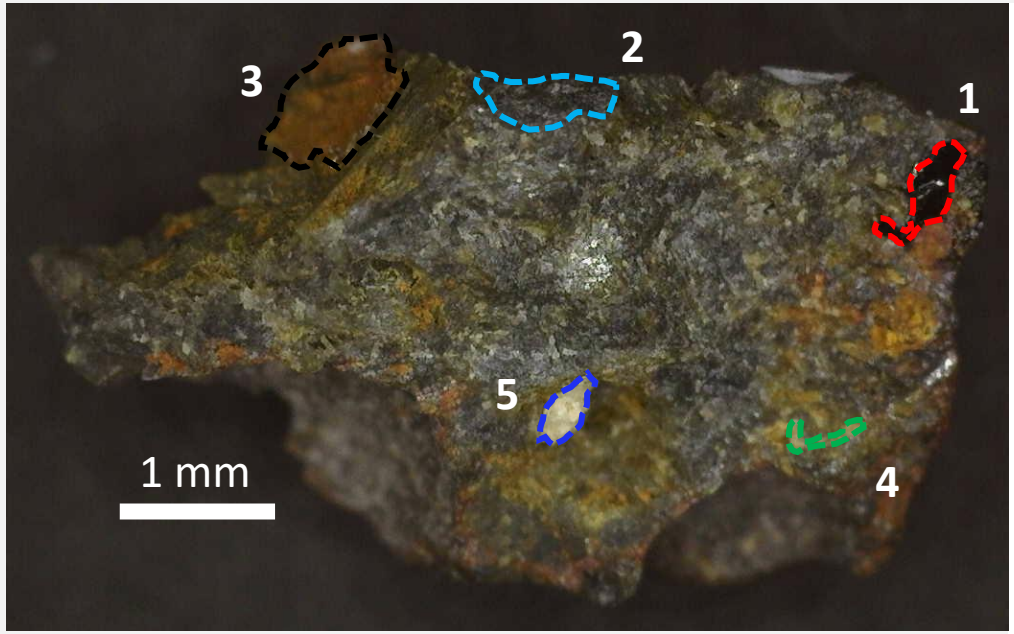

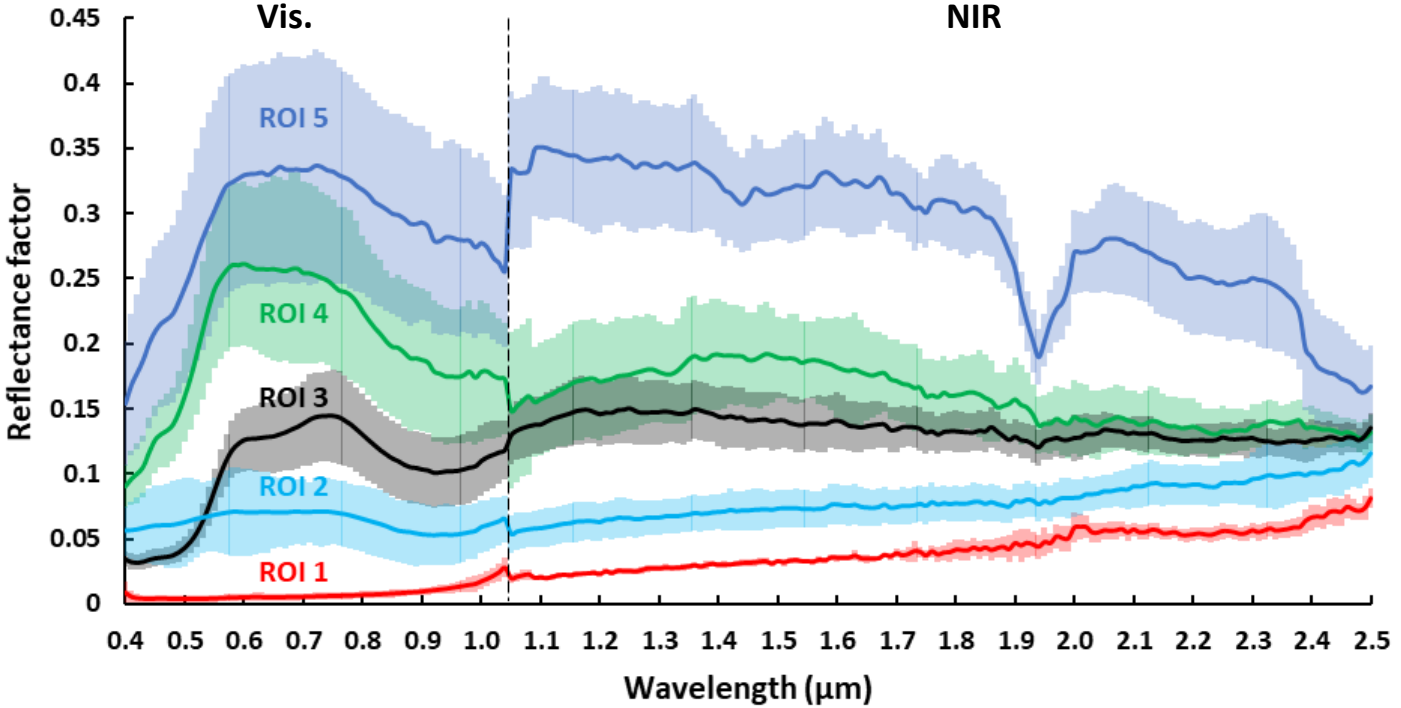

ROI 1: **glass inclusion** (very low reflectance, absence of absorption features, consistent with an amorphous opaque phase)
ROI 2: **plagioclase** (relatively featureless with higher reflectance levels)
ROI 3: likely a **mixture** of **pyroxene** and **basaltic mesostasis** (narrow absorption features at ~1.0 and ~2.0 µm)
ROI 4: **olivine** (broad absorption features near 0.9, 1.0, and 1.3 µm)
ROI 5: **pyroxene** (broad absorption features, each centred around 0.95 µm and 1.95 µm)

Next Steps

- Volume extraction (glassy inclusions, aggregates, porous spaces, etc.).
- Data pipeline optimisation and training of a model for automatic segmentation of inclusions of interest using machine learning in Dragonfly3D.
- Potential incorporation of Microscopy Imaging Center (MIC) at the University of Bern about using **UV fluorescence microscopy** to provoke the excitation of the nanoglobules within carbonaceous samples (Clemett et al., 2024 and 2025) for large-scale detection of nanoglobules within carbonaceous materials using a Zeiss AxioZoom V16 fluorescence microscope.
- Requests for **rare and precious samples will require less material to be destroyed**, resulting in a higher success chance of a successful application and future studies on a singular sample.

False-colour 3D rendering of the exterior of the Nakhla sample

E-mail: pierre-etienne.martin@unibe.ch

Dr. Pierre-Etienne M. C. MARTIN

Astronomical Institute of the Romanian Academy Scientific Seminar

28th of January 2026

PlanetS
National Centre of Competence in Research

Schweizerischer Nationalfonds

What's that Space Rock?

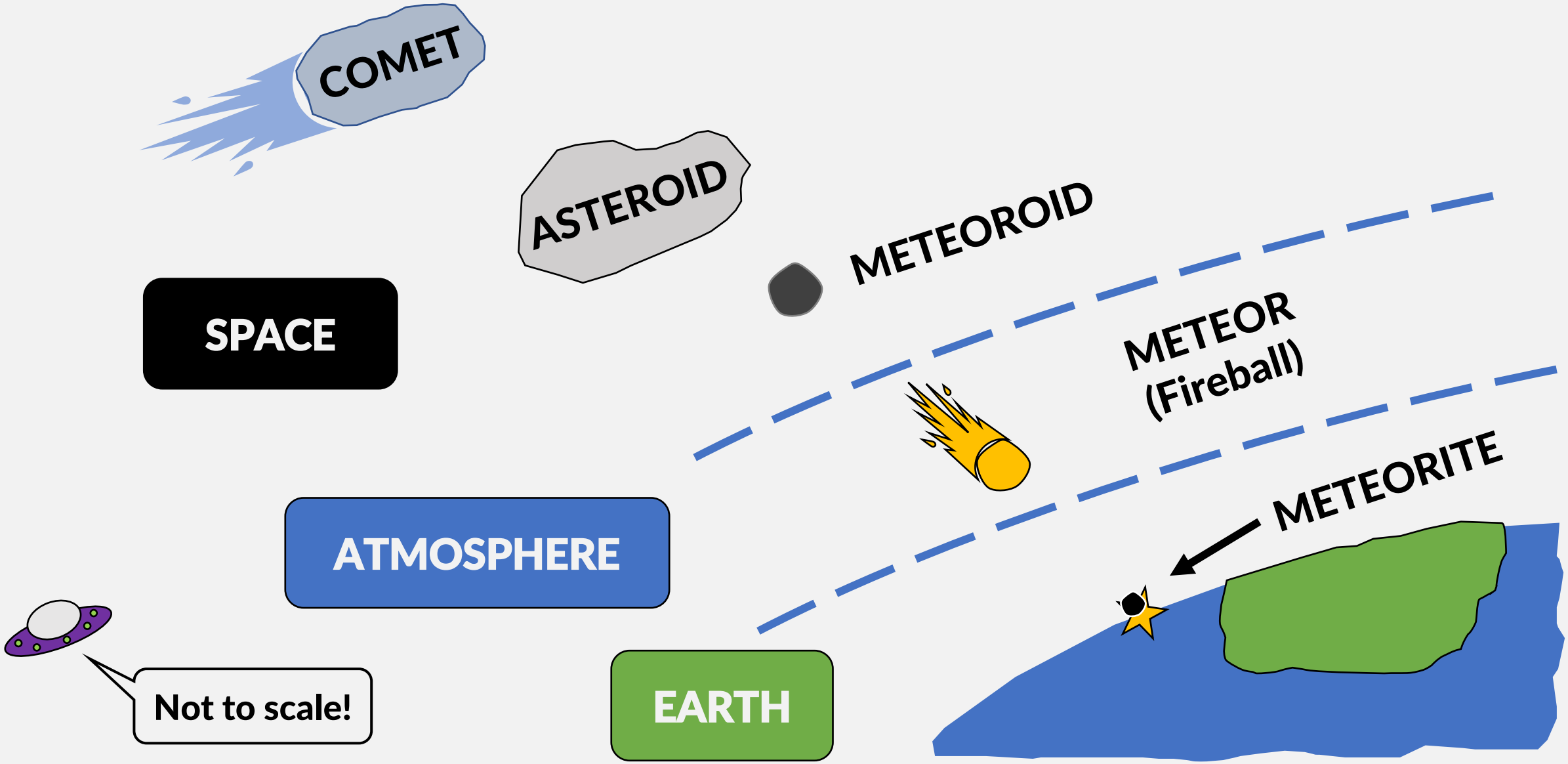

CAI Classification – Simple Inclusions

- Simple inclusions are mainly composed of spinel and comprise inclusions, fragments and/or single crystals.
- These inclusions can be in direct contact with the matrix or seldom enclosed within a pyroxene rim or mantled by Fe-rich phyllosilicates.
- Perovskite and hibonite can occur as mineral accessories alongside and seldom within the spinel.

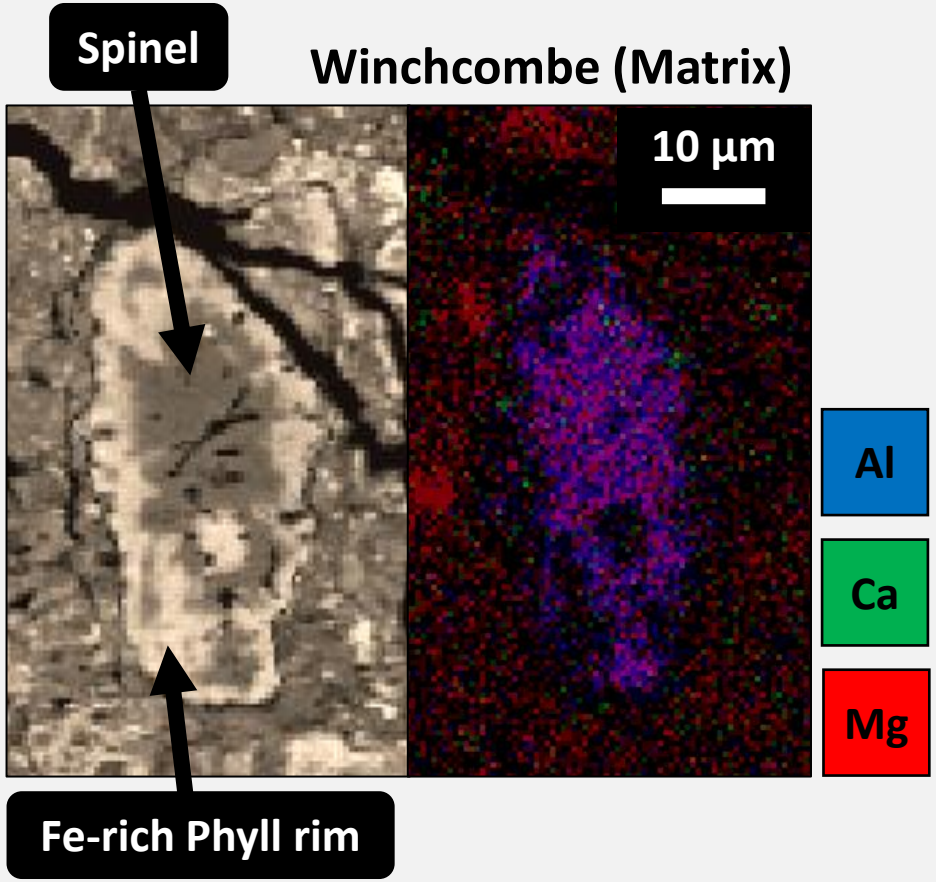

CAI Classification – Simple Aggregates

- Simple aggregates can be identified as loosely connected and porous clusters of spinel or as distended chain-like structures mostly consisting of spinel within a rim of pyroxene, olivine or phyllosilicates.

- In LAP 02239 (CM2.4-2.5), many of these objects display a pyroxene rim with 120° triple-junction grain boundaries.

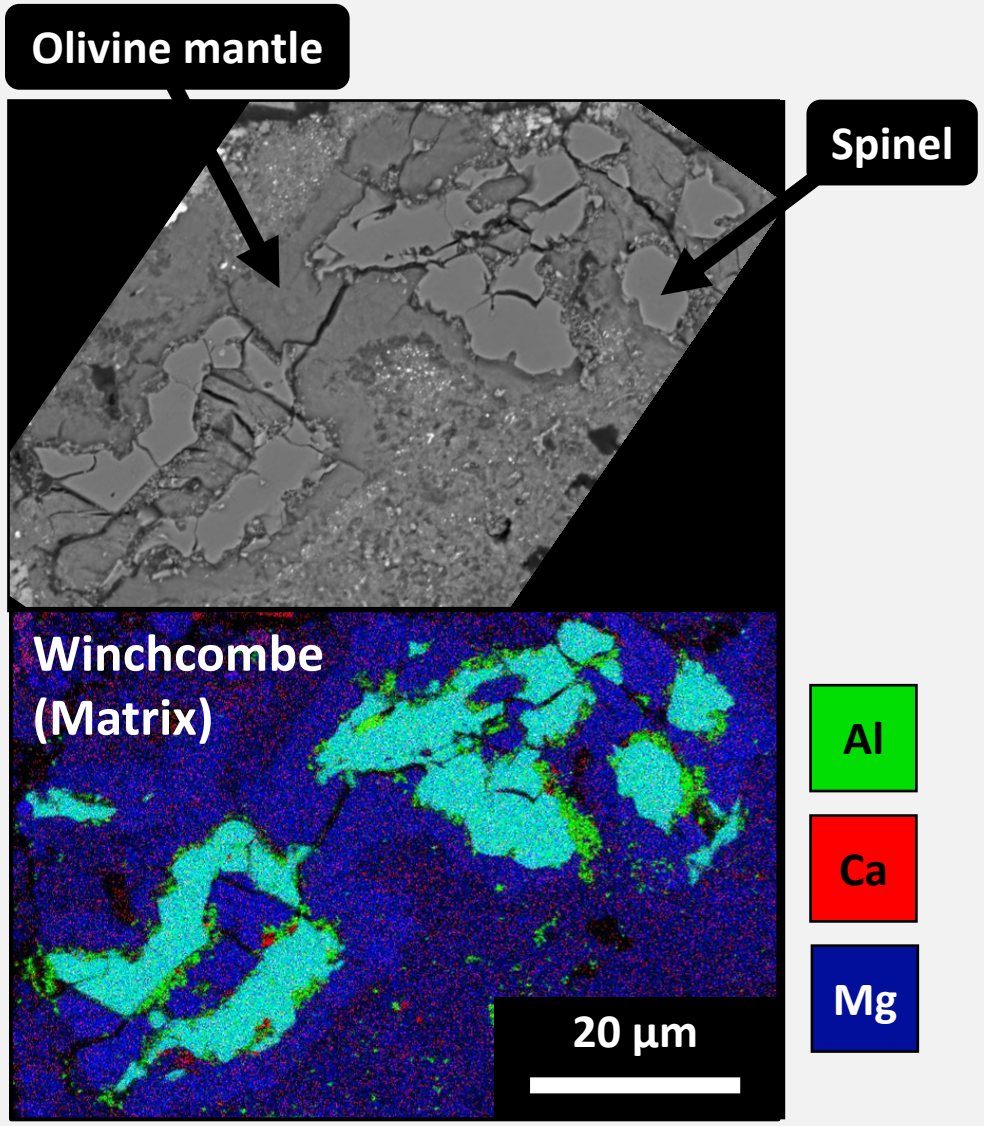

BSE and EDS maps provided by Dr. Harrison, NHM (London)

CAI Classification – Complex Aggregates

- Defined as several disjointed grains enclosed within a common pyroxene rim or phyllosilicate mantle.
- Variety of textures and phase assemblages with distinct regions and irregularly-shaped clusters.
- Several large complex aggregates (> 50 μm^2) within the most aqueously altered CM lithologies display evidence of fluid-driven mineral alteration and replacement (e.g. calcitisation)